MATCHING COMPLEXES OF TREES AND APPLICATIONS OF THE MATCHING TREE ALGORITHM

MARIJA JELIĆ MILUTINOVIĆ, HELEN JENNE, ALEX MCDONOUGH, AND JULIANNE VEGA

ABSTRACT. A matching complex of a simple graph G is a simplicial complex with faces given by the matchings on G. The topology of matching complexes is mysterious; there are few graphs for which the homotopy type is known. Marietti and Testa showed that matching complexes of forests are contractible or homotopy equivalent to a wedge of spheres. For a specific family of trees known as caterpillar graphs, we give explicit formulas for the number of spheres in each dimension. In cases where the homotopy type is more difficult to determine, a tool from discrete Morse theory called the *Matching Tree Algorithm* can be used to give bounds on the rank of non-trivial homology groups. In particular, we use the Matching Tree Algorithm to study the connectivity of honeycomb graphs, partially answering a question raised by Jonsson.

1. INTRODUCTION

Let G be a simple graph without isolated vertices that has vertex set $V(G)$ and edge set $E(G)$. An *(abstract) simplicial complex* Δ is a collection of subsets of a finite set X such that:

(i) $\emptyset \in \Delta$, and

(ii) if $\sigma \in \Delta$ and $\tau \subseteq \sigma$, then $\tau \in \Delta$.

The *dimension of a complex*, dim, is the maximum of the dimensions of its simplices.

The *matching complex* of a graph G, denoted $M(G)$, is a simplicial complex with vertices given by the edges of G and faces given by matchings contained in G, where a *matching* is a collection of pairwise disjoint edges of G. We denote an edge in G as $\overline{e} \in E(G)$ and the corresponding vertex in the matching complex of G as $e \in M(G)$; see Figure 1. We will study matching complexes of polygonal line tilings and caterpillar graphs and make use of the fact that the matching complex of a graph G is the same as the *independence complex* of the *line graph* of G. The *independence complex* of a graph G is the simplicial complex with vertex set $V(G)$ and faces given by sets of pairwise non-adjacent vertices in G. The *line graph* $L(G)$ is the graph with vertex set $E(G)$ with two vertices in $L(G)$ adjacent if and only if the corresponding edges are incident in G, where two edges in a graph are *incident* if they share a common vertex.

Matching complexes have a robust history and have been studied using both combinatorial and topological methods. In 1992, Bouc [6] introduced the matching complex of the complete graph K_n in relation to the Brown complex, $\Delta(S_p(G))$ and the Quillen complex, $\Delta(A_p(G))$, first studied in [10, 11, 29]. Here, $\Delta(P)$ is the order complex of a poset P, $S_p(G)$ is the poset of non-trivial p-subgroups of a finite group G, and $A_p(G)$ is a subposet of $S_p(G)$ consisting of all nontrivial elementary abelian p-subgroups of G. In this paper, Bouc determined how the representation of the symmetric group on the homology of $M(K_n)$ decomposes into irreducible representations. An immediate consequence of this theorem is a combinatorial formula for the Betti numbers of $M(K_n)$.
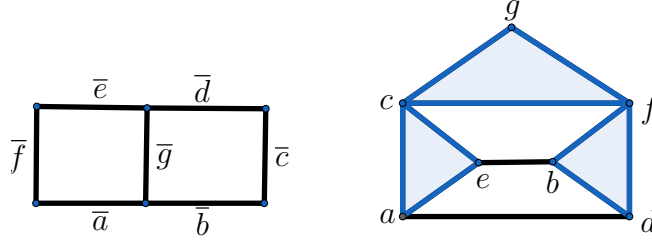
FIGURE 1. On the left we have a 2×3 grid graph, G. On the right is the corresponding matching complex $M(G)$. The vertices of $M(G)$ are given by the edges of G. There are two maximal 1-simplices (i.e. (e, b) and (a, d)) and three shaded maximal 2-simplices.

Bouc's results were the start of an extensive study of the full matching complex, $M(K_n)$, which has interesting applications (see [33]). For example, an application to the representation theory of the symmetric group S_n includes giving a representation theoretic interpretation of one of Littlewood's symmetric function identities. Most of the results about the matching complex $M(K_n)$ have analogues for the *chessboard complex*, $M(K_{m,n})$. First introduced in Garst's thesis [17], the chessboard complex aided in the analysis of Tits coset complexes.

Prior to Friedman and Hanlon's formula for the Betti numbers of $M(K_{m,n})$ [16], Ziegler [36] proved that $M(K_{m,n})$ is vertex decomposable when $2m-1 \leq n$. Consequently, $M(K_{m,n})$ is homotopy equivalent to a wedge of $(m-1)$-dimensional spheres when $2m - 1 \leq n$. In addition to homology and homotopy type, the connectivity of $M(K_n)$ and $M(K_{m,n})$ has been studied. A topological space is *k-connected* if the higher homotopy groups π_ℓ vanish for all dimensions $\ell \leq k$. The study of the connectivity of the chessboard complex [4, 30] was originally motivated by problems in computational geometry [32].

Few other families of graphs have been as well-studied as K_n and $K_{m,n}$. In [24], Kozlov used vertex decomposability to show that the matching complex of a path P_n on n vertices is either homotopy equivalent to a point if $n \equiv 2 \pmod 3$ or a sphere of dimension $\lceil \frac{n-4}{3} \rceil$ otherwise [24, Proposition 4.6]. Using similar methods, Kozlov showed that the homotopy type of the matching complex of a cycle C_n is either a sphere of dimension $\lceil \frac{n-4}{3} \rceil$ if $n \not\equiv 0 \pmod 3$ or a wedge of two spheres of dimension $\lceil \frac{n-4}{3} \rceil$ otherwise [24, Proposition 5.2]. In [9], Braun and Hough used discrete Morse matchings to find bounds on the location of non-trivial homology groups for the $2 \times n$ grid graph. Matsushita built on their results, using purely topological methods to show that the matching complex of a $2 \times n$ grid graph is homotopy equivalent to a wedge of spheres [28]. In 2008, Marietti and Testa proved that the matching complex of a forest is either contractible or homotopy equivalent to a wedge of spheres [27, Theorem 4.13].

In [21], Jonsson proposes studying the topological properties of the matching complexes of honeycomb graphs. A $r \times s \times t$ *honeycomb graph* is a hexagonal tiling that is the dual graph to a hexagonal region of equilateral triangles in which r is the length of the lower left side, s is the length of the upper left side, and t is the width of the top (Figure 2).

Historically, *perfect matchings* of the honeycomb graph have been studied because of their connections to chemistry, where they are known as Kekulè structures [22, 19], and plane

partitions [31, 25]. A *perfect matching* of a graph is a matching in which every vertex is incident to exactly one edge of the matching. In a honeycomb graph, a perfect matching corresponds to a rhombus tiling of a hexagonal region of triangles, which is equivalent to a plane partition. A *plane partition* is a two dimensional array of integers that are non-increasing moving from left to right and from top to bottom. Plane partitions can be visualized as a pile of unit cubes in the positive octant of $\mathbb{R}^3$ following the non-increasing conditions (Figure 3).
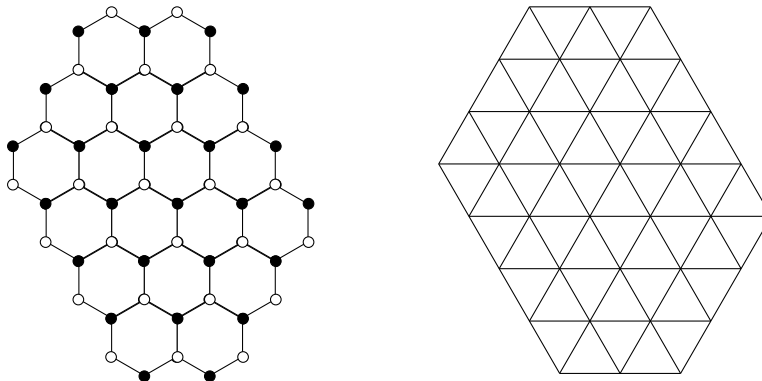

FIGURE 2. A $4 \times 3 \times 2$ honeycomb graph (left), which is the dual graph to the hexagonal region of triangles shown (right).
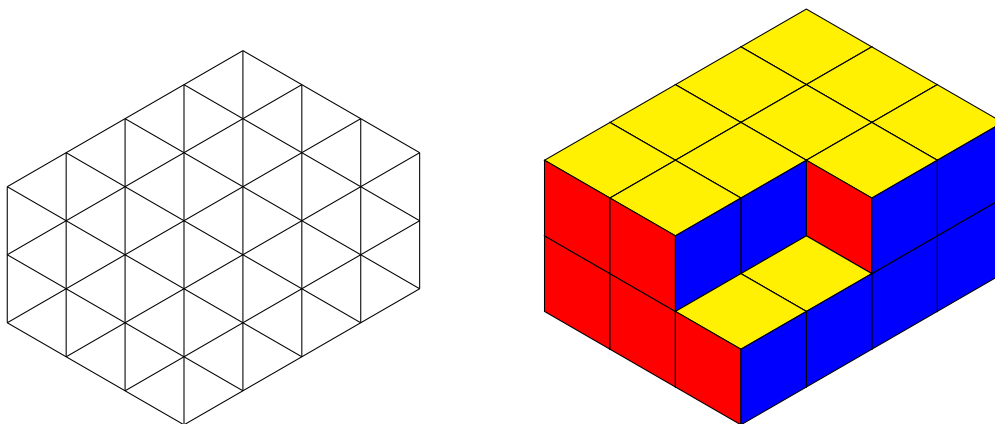

FIGURE 3. If we tile a hexagonal region of triangles (left) with rhombi, we have a plane partition (right). Shown above is the plane partition $((2,2,2),(2,2,2),(2,2,1),(2,2,1))$.

Many techniques from different areas of mathematics have been used to study matching complexes (see [33] for a thorough survey). Examples include discrete Hodge theory and symmetric function theory [16], techniques from algebraic topology such as long exact sequences [6], shellability of face posets [30, 35], combinatorial topology [27], and, more recently, discrete Morse matchings [9]. For an independence complex, discrete Morse matchings can be found through the Matching Tree Algorithm developed by Bousquet-Melou, Linusson, and Nevo [7]. We use the Matching Tree Algorithm as a tool for studying the matching complex of G after first finding the line graph of G.

Most results of matching complexes focus on understanding the homology and connectivity, see for example [4, 30, 36]. For a deeper review we refer the interested reader to [21, Chapter 11]. Determining the homotopy type of matching complexes has proven to be more difficult. Beyond Kozlov's results for paths and cycles, Matsushita's recent result for grid graphs, and Marietti's and Testa's result for forests, the literature concerning homotopy type of matching complexes is sparse.

1.1. Our Contributions.
In this paper, we explore the matching complexes of trees and certain polygonal tilings. To do so we use both combinatorial methods, namely discrete Morse matchings, as well as purely topological methods. In Section 2, we provide all of the background needed for our results, including a detailed description of the Matching Tree Algorithm in Section 2.2.

Before examining specific families of graphs, we look at general properties of matching complexes and restrictions that naturally arise on these complexes in Section 3. In Section 4, we use discrete Morse matchings to find upper and lower bounds on the dimensions of critical cells for the homotopy type of a line of polygons (Theorem 4.1) which provides partial results for honeycomb graphs. Further, we give bounds on the dimensions of critical cells for $2 \times 1 \times t$ honeycomb graphs (Theorem 4.8).

In Section 5, we build on a result by Marietti and Testa that shows the matching complex of any forest is either contractible or homotopy equivalent to a wedge of spheres (Theorem 5.1 [27, Theorem 4.13]) by using operations from Section 2.3 to determine the explicit homotopy type for general caterpillar graphs (Theorem 5.11 and Theorem 5.17). For a large class of caterpillar graphs, the number of spheres in each dimension has a nice combinatorial interpretation. When the number of spheres does not have a nice formula, we can still determine the explicit homotopy type inductively (Theorem 5.13). In Section 6, we give a connectivity bound for perfect binary trees (Proposition 6.6) and conclude with several open questions.

2. Background

2.1. Discrete Morse Theory.
Discrete Morse Theory is a tool that was developed by Forman [15] as a way to find the homotopy type of complexes by pairing faces of the complex. The pairings form a sequence of *collapses* on the complex, resulting in a homotopy equivalent cell complex.

Definition 2.1. A *partial matching* in a poset P is a partial matching on the underlying graph of the Hasse diagram of P. In other words, it is a subset $M \subseteq P \times P$ such that:

- $(a, b) \in M$ implies $a \prec b$ and
- each $a \in P$ belongs to at most one element in M.

When $(a, b) \in M$, we write $a = d(b)$ and $b = u(a)$.
A partial matching is *acyclic* if there does not exist a cycle

$$a_1 \prec u(a_1) \succ a_2 \prec u(a_2) \succ \cdots \prec u(a_m) \succ a_1$$

with $m \geq 2$ and all $a_i \in P$ distinct.

Given an acyclic partial matching M on a poset P, we call an element *critical* if it is unmatched. If every element is matched by M, M is called *perfect*. The main theorem of discrete Morse theory [23] captures the effect of acyclic matchings.

Theorem 2.2. *Let Δ be a polyhedral cell complex and let M be an acyclic matching on the face poset of Δ. Let c_i denote the number of critical i-dimensional cells of Δ. The space Δ is homotopy equivalent to a cell complex Δ_c with c_i cells of dimension i for each $i \geq 0$, plus a single 0-dimensional cell in the case where the empty set is paired in the matching.*

2.2. **Matching Tree Algorithm (MTA).** Let G be a simple graph with vertex set $V(G)$. The Matching Tree Algorithm, due to Bousquet-Melou, Linusson, and Nevo [7], is a process which constructs a discrete Morse matching on $\Sigma(\mathrm{Ind}(G))$, the face poset of the independence complex of G. The *face poset* is defined to be the poset of nonempty faces ordered by inclusion. We shorten $\Sigma(\mathrm{Ind}(G))$ to Σ when G is clear. Bousquet-Melou, Linusson, and Nevo motivate their algorithm with the following observation. One way to find a matching of Σ is to pick a vertex $v \in V(G)$ with set of neighbors $N(v)$, and then take as the matching all the pairs $(I, I \cup \{v\})$ for each $I \in \Sigma$ such that $I \cap N(v) = \emptyset$. There may be many unmatched elements, since any element of Σ that has nonempty intersection with $N(v)$ will not be in the matching. Choose one of these vertices, and repeat this process as many times as possible. This matching procedure gives rise to a rooted tree, called a matching tree of Σ, whose nodes keep track of unmatched elements at each step.

The Matching Tree Algorithm generates a matching tree of Σ, which is a binary tree whose nodes are either $\emptyset$ or of the form:

$$\Sigma(A, B) = \{I \in \Sigma : A \subseteq I \text{ and } B \cap I = \emptyset\}$$

where $A, B \subset V(G)$ with $A \cap B = \emptyset$. Our version of the Matching Tree Algorithm is modified from its presentation in Braun and Hough [9] (see Remark 2.3).

Matching Tree Algorithm. Beginning with the root node $\Sigma(\emptyset, \emptyset)$, at each node $\Sigma(A, B)$ where $A \cup B \neq V(G)$ apply the following procedure:
  (1) If there is a vertex $v \in V(G) \setminus (A \cup B)$ such that $N(v) \setminus (A \cup B) = \emptyset$ then v is called a *free vertex*. Give $\Sigma(A, B)$ a single child labeled $\emptyset$.
  (2) Otherwise, if there is a vertex $v \in V \setminus (A \cup B)$ such that $N(v) \setminus (A \cup B)$ is a single vertex w, then v is called a *pivot* and w is called a *matching vertex*. Give $\Sigma(A, B)$ a single child labeled $\Sigma(A \cup \{w\}, B \cup N(w))$.
  (3) When there is no vertex that satisfies (1) or (2) and $A \cup B \neq V(G)$, we call $\Sigma(A, B)$ *split ready* and the graph induced by $V(G) \setminus (A \cup B)$ a *configuration*. We choose any vertex $v \in V(G) \setminus (A \cup B)$, which we call the *splitting vertex*. Give $\Sigma(A, B)$ two children: $\Sigma(A \cup \{v\}, B \cup N(v))$, which we call the *right child*, and $\Sigma(A, B \cup \{v\})$, which we call the *left child*.

Remark 2.3. The algorithm as presented in [9] allows one to do steps (1),(2), and (3) in any order, but we found that our ordering worked well for our purposes. Note that when any ordering is allowed, if w is a matching vertex with respect to pivot v, we could do either step (2) or step (3). If we choose w as a splitting vertex, $\Sigma(A, B \cup \{w\})$ has v as a free vertex and therefore will have the unique child $\emptyset$. Thus, the only remaining child is $\Sigma(A \cup \{w\}, B \cup N(w))$, as in step (2).

We have the following theorem which is due to Bousquet-Melou, Linusson, and Nevo, but is stated below as it appears in Braun and Hough [9].

Theorem 2.4. *A matching tree for G yields an acyclic partial matching on the face poset of $\mathrm{Ind}(G)$ whose critical cells are given by the non-empty sets $\Sigma(A, B)$ labeling non-root leaves*
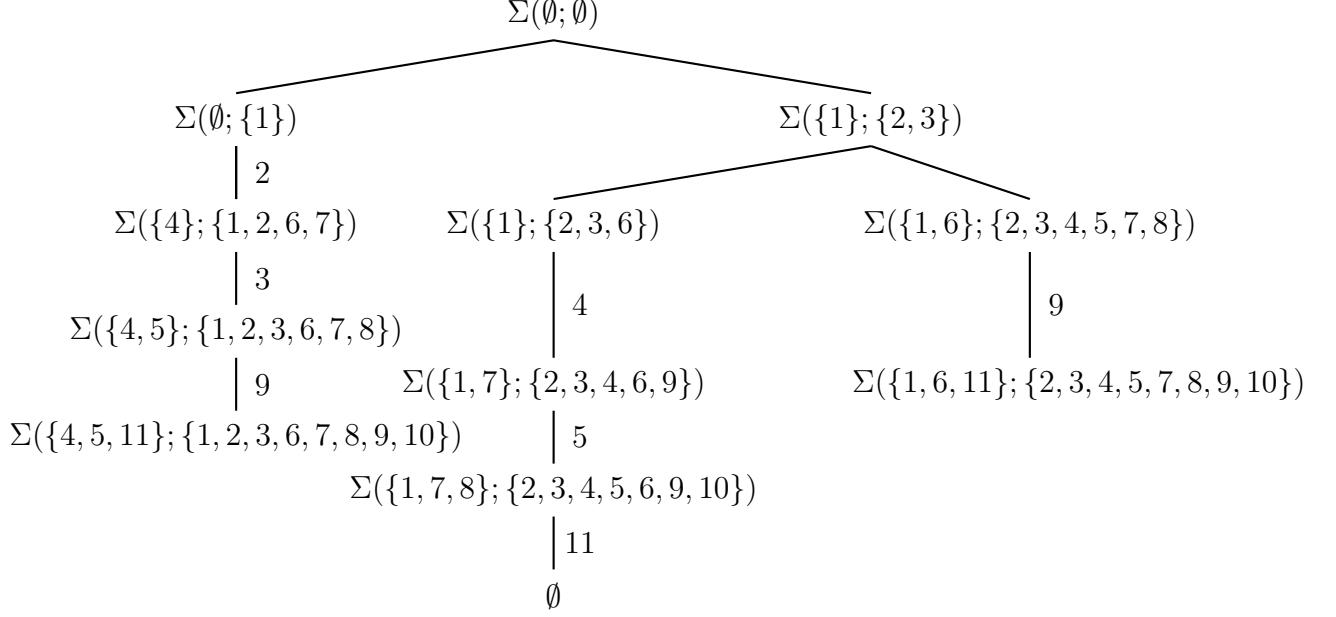
$$\Sigma(\emptyset; \emptyset)$$

$$\Sigma(\emptyset; \{1\}) \qquad\qquad \Sigma(\{1\}; \{2,3\})$$

$$\Big| \, 2$$

$$\Sigma(\{4\}; \{1,2,6,7\}) \qquad \Sigma(\{1\}; \{2,3,6\}) \qquad\qquad \Sigma(\{1,6\}; \{2,3,4,5,7,8\})$$

$$\Big| \, 3 \qquad\qquad\qquad\qquad \Big| \, 4 \qquad\qquad\qquad\qquad\qquad \Big| \, 9$$

$$\Sigma(\{4,5\}; \{1,2,3,6,7,8\})$$

$$\Big| \, 9 \qquad \Sigma(\{1,7\}; \{2,3,4,6,9\}) \qquad\qquad \Sigma(\{1,6,11\}; \{2,3,4,5,7,8,9,10\})$$

$$\Sigma(\{4,5,11\}; \{1,2,3,6,7,8,9,10\}) \qquad \Big| \, 5$$

$$\Sigma(\{1,7,8\}; \{2,3,4,5,6,9,10\})$$

$$\Big| \, 11$$

$$\emptyset$$

FIGURE 4. The tree resulting from applying the Matching Tree Algorithm to the graph in Example 2.5. The pivot or free vertex at each step is labeled.

of the matching tree. In particular, for such a set $\Sigma(A, B)$, the set A yields a critical cell in $Ind(G)$.

Example 2.5. Let G be the $1 \times 1 \times 2$ honeycomb graph, whose line graph $L(G)$ is shown below:
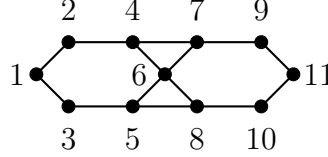
$\Sigma(\emptyset, \emptyset)$ is split ready so we must choose a splitting vertex. Choosing 1 produces two children, $\Sigma(\emptyset, \{1\})$ and $\Sigma(\{1\}, \{2,3\})$, as shown in Figure 4. We first consider the left child. Since 4 is the only neighbor of 2 outside of $\{1\}$, we use 4 as a matching vertex with respect to the pivot 2. This gives $\Sigma(\emptyset, \{1\})$ one child that we label $\Sigma(\{4\}, \{1,2,6,7\})$. Similarly, we use 5 as a matching vertex with respect to the pivot 3, obtaining the child $\Sigma(\{4,5\}, \{1,2,3,6,7,8\})$. Finally, we use 11 as a matching vertex, concluding this branch of the tree with the node

$$\Sigma(\{4,5,11\}, \{1,2,3,6,7,8,9,10\}).$$

The $\Sigma(\{1\}, \{2,3\})$ branch of the tree is split ready. Choosing 6 as splitting vertex and continuing the algorithm produces the matching tree shown in Figure 4. The resulting matching tree has three leaf nodes:

$$\emptyset, \ \Sigma(\{1,6,11\}, \{2,3,4,5,7,8,9,10\}), \ \text{and} \ \Sigma(\{4,5,11\}, \{1,2,3,6,7,8,9,10\}).$$

We have two nonempty leaf nodes, which correspond to two critical cells that each have three elements. Since $M(G)$ has two critical cells of dimension 2 and one cell of dimension 0, by Theorem 2.2, $M(G) \simeq S^2 \vee S^2$. In this example we were able to determine the homotopy

6

type of $M(G)$ from the Matching Tree Algorithm because the critical cells were all of the same dimension. In general this will not always be the case, but we do always get homological information because if no critical cells appear of a given dimension, then the homology in this dimension must be trivial.

We call the process of applying (1) and (2) from the Matching Tree Algorithm to $\Sigma(A, B)$ until we reach a split ready descendant *split preparing*. In Example 2.5, when split preparing $\Sigma(\emptyset, \{1\})$, we used 4, then 5, and then 11 as matching vertices. We could have used 5 as a matching vertex before using 4. We show in the next lemma that the process of split preparing has no effect on the size of the resulting critical cells.

Lemma 2.6. *Let G be a graph and let $\Sigma(A, B)$ be a leaf of a matching tree of G. If $\Sigma(\hat{A}, \hat{B})$ and $\Sigma(\tilde{A}, \tilde{B})$ are two split ready leaves obtained from split preparing $\Sigma(A, B)$, then $\Sigma(\hat{A}, \hat{B}) = \emptyset$ if and only if $\Sigma(\tilde{A}, \tilde{B}) = \emptyset$ and otherwise $|\hat{A}| = |\tilde{A}|$ and $\hat{A} \cup \hat{B} = \tilde{A} \cup \tilde{B}$.*

Proof. For a set of vertices S, let $\overline{N}(S) := \bigcup_{v \in S} \overline{N}(v)$, where $\overline{N}(v) := v \cup N(v)$. If the lemma does not hold, then we must be able to satisfy one of three conditions:

(1) $\Sigma(\hat{A}, \hat{B}) = \emptyset$ but $\Sigma(\tilde{A}, \tilde{B}) \neq \emptyset$,
(2) $|\hat{A}| \neq |\tilde{A}|$, or
(3) $\hat{A} \cup \hat{B} \neq \tilde{A} \cup \tilde{B}$.

We can assume without loss of generality that $A = B = \emptyset$. For one of these conditions to be true, there exists vertex minimal graph G such that $v_1, \ldots, v_k$ and $\tilde{v}_1, \ldots, \tilde{v}_h$ are sequences of vertices with the following properties:

(a) For each i, v_i is a matching vertex of $V(G) \setminus \overline{N}(\{v_1, \ldots, v_{i-1}\})$ and $\tilde{v}_i$ is a matching vertex of $V(G) \setminus \overline{N}(\{\tilde{v}_1, \ldots, \tilde{v}_{i-1}\})$.
(b) $V(G) \setminus \overline{N}(\{v_1, \ldots, v_k\})$ and $V(G) \setminus \overline{N}(\{\tilde{v}_1, \ldots, \tilde{v}_h\})$ contain no matching vertices.
(c) $V(G) \setminus \overline{N}(\{\tilde{v}_1, \ldots, \tilde{v}_h\})$ contains no free vertices.
(d) If $V(G) \setminus \overline{N}(\{v_1, \ldots, v_k\})$ contains no free vertices, then $k \neq h$ or $V(G) \setminus \overline{N}(\{v_1, \ldots, v_k\}) \neq V(G) \setminus \overline{N}(\{\tilde{v}_1, \ldots, \tilde{v}_h\})$.

To see why these properties must hold, note that $v_1, ..., v_k$ and $\tilde{v}_1, ..., \tilde{v}_h$ are both maximal lists of vertices that can be added to A while split preparing (by properties (a) and (b)). Once there are no more matching vertices, we check for free vertices. If both $V(G) \setminus \overline{N}(\{v_1, \ldots, v_k\})$ and $V(G) \setminus \overline{N}(\{\tilde{v}_1, \ldots, \tilde{v}_h\})$ have a free vertex, we cannot satisfy any of the three conditions, justifying property (c). If only one of them has a free vertex, we satisfy condition (1). If neither has a free vertex, then we need either $k \neq h$ to satisfy condition (2) or $V(G) \setminus \overline{N}(\{v_1, \ldots, v_k\}) \neq V(G) \setminus \overline{N}(\{\tilde{v}_1, \ldots, \tilde{v}_h\})$ to satisfy condition (3).

We will show by contradiction that these properties cannot all hold. By definition of matching vertices, there must be some pivot p such that $N(p) = \{v_1\}$. If $v_1 = \tilde{v}_i$ for some i, then we can reorder $(\tilde{v}_1, \ldots, \tilde{v}_h)$ by placing $\tilde{v}_i$ at the beginning without changing $V(G) \setminus \overline{N}(\{\tilde{v}_1, \ldots, \tilde{v}_h\})$. This means that the sequences $v_2, \ldots, v_k$ and $\tilde{v}_1, \ldots, \tilde{v}_{i-1}, \tilde{v}_{i+1}, \ldots, \tilde{v}_h$ would satisfy the above properties on the graph $G \setminus (\overline{N}(v_1))$, contradicting the minimality of G.

If $v_1 \notin \{\tilde{v}_1, \ldots, \tilde{v}_h\}$ then there must be some minimal i such that p is not a pivot in $V(G) \setminus \overline{N}(\{\tilde{v}_1, \ldots, \tilde{v}_i\})$. This means at least one of $\{p, v_1\}$ is in $\overline{N}(\{\tilde{v}_1, \ldots, \tilde{v}_i\})$ and not in $\overline{N}(\{\tilde{v}_1, \ldots, \tilde{v}_{i-1}\})$. This is only possible if (i) $p = \tilde{v}_i$, (ii) $v_1 = \tilde{v}_i$, (iii) $p \in N(\tilde{v}_i)$, or (iv) $v_1 \in N(\tilde{v}_i)$.

7

We have already ruled out (ii); since $N(p) = \{v_1\}$, (iii) is the same as (ii); and (iv) would make p a free vertex. Thus, we only need to consider (i), where $p = \tilde{v}_i$.

If $p = \tilde{v}_i$, then $N(v_1) = \{p\}$ is in $V(G) \setminus \overline{N}(\{\tilde{v}_1, \ldots, \tilde{v}_{i-1}\})$. Since p is a pivot with respect to v_1, $N(p) = \{v_1\}$ is also in $V(G) \setminus \overline{N}(\{\tilde{v}_1, \ldots, \tilde{v}_{i-1}\})$. This means that

$$\overline{N}(\{\tilde{v}_1, \ldots, \tilde{v}_{i-1}, p, \tilde{v}_{i+1}, \ldots, \tilde{v}_h\}) = \overline{N}(\{\tilde{v}_1, \ldots, \tilde{v}_{i-1}, v_1, \tilde{v}_{i+1}, \ldots, \tilde{v}_h\}).$$

Then, we can reorder $\tilde{v}_1, \ldots, \tilde{v}_{i-1}, v_1, \tilde{v}_{i+1}, \ldots, \tilde{v}_h$ so that v_1 comes first which leads to the contradiction of the minimality of G as before.

$\square$

Remark 2.7. While the process of split preparing has no affect on the size of the resulting critical cells, our choice of splitting vertices affects both the efficiency of the algorithm and the resulting critical cells. The Matching Tree Algorithm will always produce a discrete Morse matching of the independence complex, but it won't always be the same discrete Morse matching. Two different discrete Morse matchings may give rise to two (homotopy equivalent) cell complexes with a different number or dimensions of cells. For this reason, our proofs in Section 4 involve careful choices of splitting vertices.

We conclude the section with a lemma that enables us to give a lower bound on the size of the critical cells of a matching complex for a general graph using the Matching Tree Algorithm.

Lemma 2.8. *Let G be a graph and let $\{v_1, \ldots, v_k\} \subseteq V(G)$ such that $\overline{N}(v_1)$, $\overline{N}(v_2)$,...., and $\overline{N}(v_k)$ are pairwise disjoint. After applying the Matching Tree Algorithm to $\Sigma(Ind(G))$ without choosing v_i as a splitting vertex for any $i \in [k]$, all resulting critical cells have at least k elements.*

Proof. Apply the Matching Tree Algorithm without choosing v_i as a splitting vertex for any $i \in [k]$. Assuming the Matching Tree Algorithm has not terminated, there exists $x \in V(G) \setminus \{v_1, \ldots, v_k\}$ that can be chosen as a splitting vertex because otherwise there is a free vertex v_i. Once the algorithm terminates, consider an arbitrary nonempty leaf node $\Sigma(A, B)$. It is possible that no such leaf node exists, in which case the result holds. The critical cell A contains at least one vertex from each $\overline{N}(v_i)$ for $i \in [k]$. If $v_i \in A$, we are done. Otherwise $v_i \in B$. Since v_i is not a splitting vertex, v_i must be a pivot with respect to some matching vertex $w_i \in N(v_i)$. Therefore, $w_i \in A$ and the result follows. $\square$

2.3. **Graph Operations.** An effective way to study the homotopy type of complexes arising from graphs is by finding a way to inductively build the graph and study the homotopy type at each step, see for example [1, 2, 13, 14, 26]. We will use this method in Section 5.1; here, we present the necessary topological background. We will state well-known topological results without proof; further detail can be found in [18].

Remark 2.9. If G and H are disjoint graphs it is clear that

$$M(G \cup H) = M(G) * M(H),$$

where $*$ denotes the *join* operation: $\Delta * \Delta' = \{\sigma \cup \sigma' : \sigma \in \Delta, \sigma' \in \Delta'\}$ for two simplicial complexes Δ and Δ'. Note that in the case where $M(H)$ is contractible, $M(G \cup H) \simeq M(G) * \text{pt} \simeq \text{pt}$.

Next, we will consider $M(G \cup H)$ in the case where G and H are two graphs that share only one vertex. If $V(G) \cap V(H) = \{x\}$, the *wedge sum* $G \underset{x}{\vee} H$ of G with H over x is the graph with vertex set $V(G) \cup V(H)$ and edge set $E(G) \cup E(H)$. The resulting matching complex is formed by taking two separate joins and *gluing* over a common subcomplex. If $A \subseteq X$ and $A \subseteq Y$, *gluing* X and Y along A, denoted $X \underset{A}{\bigcup} Y$, is identifying the common subcomplex A. For a rigorous review of topological gluing refer to [18].

Lemma 2.10. *Let G and H be graphs with one common vertex x. Then we have the following decomposition of the matching complex of the wedge sum $G \underset{x}{\vee} H$:*

$$M(G \underset{x}{\vee} H) \;=\; M(G \smallsetminus x) * M(H) \underset{M(G \smallsetminus x)*M(H \smallsetminus x)}{\bigcup} M(G) * M(H \smallsetminus x).$$

Proof. An edge $e \in E(G)$ is incident to an edge in H if and only if x is an endpoint of e. In the graph $G \smallsetminus x$, all of the edges incident to H are deleted, leaving two disjoint graphs $G \smallsetminus x$ and H. Hence by Remark 2.9, $M((G \smallsetminus x) \cup H) = M(G \smallsetminus x) * M(H)$. Similarly, $M((H \smallsetminus x) \cup G) = M(H \smallsetminus x) * M(G)$. Now, we glue along the common faces, which are the faces that do not contain any of the edges that have x as an endpoint. Thus we glue along the subcomplex $M(G \smallsetminus x) * M(H \smallsetminus x)$.

$\square$

For a space X, the *suspension SX* is the quotient of $X \times I$ under the identifications $(x_1, 0) \sim (x_2, 0)$ and $(x_1, 1) \sim (x_2, 1)$ for all $x_1, x_2 \in X$. A suspension is homeomorphic to the join of X with two points $\{a, b\}$. The *cone CX* of a space X is $(X \times I)/(X \times \{0\})$ and is homeomorphic to the join of X with one point.

Remark 2.11. The following properties of suspension and wedge are well-known, see [34, 12, 18].

(1) Let $f : X \to X'$ and $g : Y \to Y'$ be two homotopy equivalences. Then the join of these maps $f * g : X * Y \to X' * Y'$ is also a homotopy equivalence.

(2) $S^m * S^n \cong S^{m+n+1}$, and more generally,

$$(S^{a_1} \vee \cdots \vee S^{a_k}) * (S^{b_1} \vee \cdots \vee S^{b_\ell}) \simeq \bigvee_{\substack{i=1,\ldots,k \\ j=1,\ldots,\ell}} S^{a_i+b_j+1}$$

(3) $S(S^m \vee S^n) \simeq S(S^m) \vee S(S^n) \cong S^{m+1} \vee S^{n+1}$, and more generally,

$$S(S^{a_1} \vee \cdots \vee S^{a_k}) \simeq \bigvee_{i=1,\ldots,k} S^{a_i+1}$$

Definition 2.12. Let G be a graph and $\overline{x} \in E(G)$. Define the *deletion* of $\overline{x}$ by

$$\mathrm{del}_G(\overline{x}) := \{\overline{e} \in E(G) \mid \overline{e} \cap \overline{x} = \emptyset\}.$$

We will abuse notation and refer to the subgraph of G spanned by the deletion of $\overline{x}$ as $\mathrm{del}_G(\overline{x})$.

Definition 2.13. We say that a graph G has an *independent m-leg, $m \geq 1$,* if there exist edges $\overline{x}_1, \overline{x}_2, \ldots, \overline{x}_m$ and $\overline{y}$ such that $\overline{x}_1, \overline{x}_2, \ldots, \overline{x}_m$ are incident as leaves to the same endpoint of $\overline{y}$ (see Figure 5).

Lemma 2.14 is a consequence of [27, Proposition 3.3].

Lemma 2.14. *Let G be a graph with an independent m-leg, as shown in Figure 5. If $G_1 = del_G(\overline{x_1})$ and $G_2 = del_G(\overline{y})$, then $M(G) \simeq \left[\bigvee_{m-1} S(M(G_1)) \right] \vee S(M(G_2))$. In particular, when $m = 1$, $M(G) \simeq S(M(G_2))$.*

Lemma 2.14 and induction can be used to recover the homotopy type for matching complexes of paths [23]. Additionally, the next example shows how the lemma can be applied to determine the homotopy type of a small family of trees.

Example 2.15. Consider the family of graphs $\{T_i\}$ where T_1 is a path of length 2 and, in general, T_i is constructed from T_{i-1} by adding a path of length 2 to the middle vertex of the most recent path added. Note that i is the number of paths of length 2 used to construct T_i. Figure 6 depicts $T_1, T_2,$ and T_3. It is easy to check that $M(T_1) \simeq S^0$, $M(T_2) \simeq S^0$, and $M(T_3) \simeq S^1$. By Lemma 2.14, $M(T_i) \simeq S(M(T_{i-2}))$. For example,

$M(T_4) \simeq S(M(T_2)) \simeq S^1$,
$M(T_5) \simeq S(M(T_3)) \simeq S^2$, and
$M(T_6) \simeq S(M(T_4)) \simeq S^2$.

In general, $M(T_n) \simeq S^k$ where $k = \lfloor \frac{n-1}{2} \rfloor$ and $n \geq 1$.
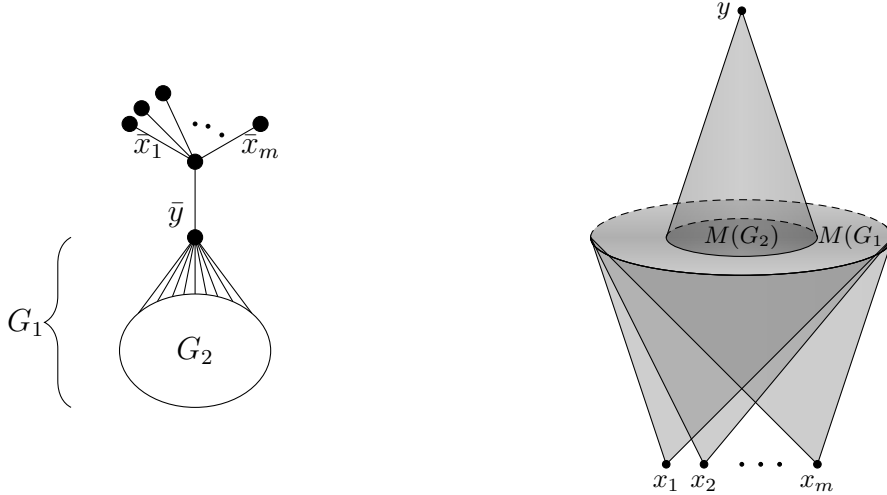
FIGURE 5. A graph G with edges $\bar{x}_1, \ldots, \bar{x}_m$ and $\bar{y}$ that form an independent m-leg. Notice that in this case, $M(G)$ is $\bigcup_{M(G_1)} \left[\bigcup_{x_i} (C^{x_i}(M(G_1))) \right] \bigcup_{M(G_2)} C^y(M(G_2))$.

3. CONNECTEDNESS AND DIAMETER

There are inherent restrictions on the types of matching complexes that arise when considering the structure of graphs. For example, Jonsson [21] gave lower bounds on the depth of $M(G)$ under certain conditions, such as in the case where G admits a perfect matching. More recently, Bayer, Goeckner, and Jelić Milutinović completely classified matching complexes that are combinatorial manifolds with and without boundaries [3]. Proposition 3.1 characterizes when the matching complex is disconnected.
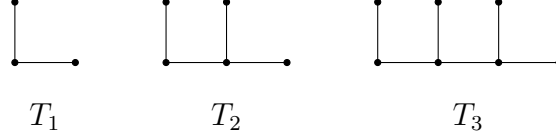
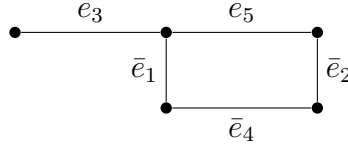FIGURE 6. The family of graphs described in Example 2.15.

FIGURE 7. The matching complex of the graph shown above is P_5, which has diameter 4.

Proposition 3.1. *Let $M(G)$ denote the matching complex of a graph G. $M(G)$ is disconnected if and only if there exists a nonempty set $S \subset E(G)$ such that $S \neq E(G)$, and every edge of $E(G) \setminus S$ is incident to every edge of S.*

Proof. ($\Leftarrow$) Assume there is a set $\emptyset \subsetneq S \subsetneq E(G)$ such that every edge of $E(G) \setminus S$ is incident to every edge of S. Then there cannot be a matching containing edges of S and edges of $E(G) \setminus S$ and thus the matching complex is disconnected.

($\Rightarrow$) Assume that there does not exist a set $\emptyset \subsetneq S \subsetneq E(G)$ such that every edge of $E(G) \setminus S$ is incident to every edge of S. Let $\bar{e}_1, \bar{e}_5 \in E(G)$. We will show that there is a path from e_1 to e_5 in the matching complex. We can assume $\bar{e}_1$ is incident to $\bar{e}_5$, since otherwise $\{\bar{e}_1, \bar{e}_5\}$ is a matching and thus there is an edge from e_1 to e_5 in the matching complex.

Let $\bar{e}_2$ be an edge not incident to $\bar{e}_1$ (which exists by assumption). We can assume that $\bar{e}_2$ and $\bar{e}_5$ are incident or e_1 and e_5 are connected by the path $\{e_1, e_2, e_5\}$ in $M(G)$. Similarly, let $\bar{e}_4$ be an edge not incident to $\bar{e}_5$. We can assume that $\bar{e}_4$ is incident to both $\bar{e}_1$ and $\bar{e}_2$,

Since $\bar{e}_4$ and $\bar{e}_5$ are each incident to both $\bar{e}_1$ and $\bar{e}_2$, these four edges form a cycle. By assumption, there is an edge $\bar{e}_3$ that is not incident to both $\bar{e}_1$ and $\bar{e}_2$ or both $\bar{e}_4$ and $\bar{e}_5$. Thus, it is incident to at most one of the 4 vertices formed by the cycle $\bar{e}_1, \bar{e}_5, \bar{e}_2, \bar{e}_4$. Checking cases shows that there is a path between e_1 and e_5 of length at most 4. $\square$

The *diameter* of a graph or 1-skeleton is the maximum over the minimum distance between any two vertices. The following corollary is immediate from the proof of Proposition 3.1.

Corollary 3.2. *There is a path of length less than or equal to 4 between any two vertices of the 1-skeleton of any connected matching complex. That is, any connected matching complex has diameter less than or equal to 4.*

This bound is achievable. For example, see Figure 7 which shows a graph with matching complex P_5, a path on five vertices.

Furthermore, the matching complexes of a large class of graphs have 1-skeletons with diameter 2.

Proposition 3.3. *If G has at least two incident edges, but no pair $\bar{e}, \bar{e}'$ such that every edge in $E(G) \setminus \{\bar{e}, \bar{e}'\}$ is incident to either $\bar{e}$ or $\bar{e}'$, then the matching complex of G has a 1-skeleton with diameter 2.*

11

Proof. For two incident edges $\overline{h_1}$ and $\overline{h_2}$ in G the distance between the two corresponding vertices h_1 and h_2 on the 1-skeleton of $M(G)$ must be at least 2. Therefore, the diameter is at least 2. Furthermore, for any pair of edges $\overline{e_1}$ and $\overline{e_2}$ in G there exists a third edge $\overline{g}$ that is not incident to either $\overline{e_1}$ or $\overline{e_2}$, so $\{e_1, g, e_2\}$ is a path in the 1-skeleton of $M(G)$ from e_1 to e_2. Hence, $M(G)$ has diameter 2. $\qquad\square$

4. POLYGON TILINGS
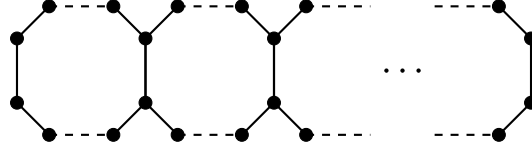
FIGURE 8. A graph of t $2n$-gons.

In [21], Jonsson proposes studying the topology of matching complexes of honeycomb graphs. In this section we will consider polygonal tilings and $2 \times 1 \times t$ honeycombs for $t \geq 1$, providing partial results for the matching complexes of honeycomb graphs.

Consider a graph of t $2n$-gons for $n \geq 2$ and $t \geq 1$ arranged in a line as shown in Figure 8. Jonsson explored the matching complex of this graph when $n = 2$, so the graph is a line of quadrilaterals [20], showing that the matching complex is at least d_t^{min}-connected, where

$$d_t^{min} = \begin{cases} 2\left\lfloor \dfrac{t-2}{3} \right\rfloor + 2 & \text{if } t \equiv 0 \ (\text{mod } 3) \\ \left\lfloor \dfrac{2t}{3} \right\rfloor & \text{otherwise} \end{cases}$$

Braun and Hough [9] gave a proof of this result using the Matching Tree Algorithm. They also showed that the matching complex of t 4-gons has no d-dimensional cells for $d > d_t^{max}$, where

$$d_t^{max} = \left\lfloor \frac{3t-1}{4} \right\rfloor$$

Matsushita [28] recently concluded the study of the matching complex of t 4-gons by determining the homotopy type.

The following theorem extends these results by considering when $n > 2$. Note that the theorem only considers when $t > 1$, since the homotopy type of matching complexes of cycle graphs are known.

Theorem 4.1. *Let $t > 1$ and $n > 2$. Define*

$$d^{\min} = \begin{cases} \dfrac{2nt}{3} - t & \text{if } n \equiv 0 \ (\text{mod } 3) \\ \dfrac{2nt+t}{3} - t & \text{if } n \equiv 1 \ (\text{mod } 3) \\ \dfrac{2nt-t}{3} - \left\lfloor \dfrac{t+1}{2} \right\rfloor & \text{if } n \equiv 2 \ (\text{mod } 3) \end{cases}$$

12

and

$$d^{\max} = \begin{cases} \dfrac{2nt}{3} - \left\lfloor \dfrac{t}{2} \right\rfloor - 1 & \text{if } n \equiv 0 \ (\text{mod } 3) \\[2ex] \dfrac{2nt + t}{3} - t & \text{if } n \equiv 1 \ (\text{mod } 3) \\[2ex] \dfrac{2nt - t}{3} - 1 & \text{if } n \equiv 2 \ (\text{mod } 3) \end{cases} \cdot$$

The matching complex of a graph of t $2n$-gons is homotopy equivalent to a space with no d-dimensional cells, where $0 < d < d^{\min}$ or $d > d^{\max}$. Consequently, the connectivity is at least $d^{\min} - 1$.

Proof. We will use the Matching Tree Algorithm to establish both bounds. Since this algorithm finds matchings on the face poset of the independence complex of a graph, we apply the algorithm to the line graph, which we label as shown in Figure 9, when $j = 1$.

Recall by Lemma 2.6 and Remark 2.7 that the size of the critical cells of our matching tree depends only on the order that we choose splitting vertices and not how we split prepare. We apply the Matching Tree Algorithm using the following procedure.

For each split ready leaf node $\Sigma(A, B)$:

> Step 1: Choose the smallest a_j not yet assigned to A or B as our splitting vertex. This produces two leaves, $\Sigma(A, B \cup \{a_j\})$ and $\Sigma(A \cup \{a_j\}, B \cup N(a_j))$.
> Step 2: Split prepare each leaf.

At Step 1 of this algorithm, there will be two possible cases for $V(G) \setminus (A \cup B)$, as seen in Figure 9 and Figure 10. We now describe the process of split preparing each leaf depending on: (i) the case, (ii) whether the leaf is the left or right child of $\Sigma(A, B)$, and (iii) the value of $n \ (\text{mod } 3)$. To do this, we define the following subsets of $V(G)$:

> $E_j = \{a_j \text{ as well as } b_{(j,k)} \text{ and } c_{(j,k)} \text{ for all } k \equiv 0 \ (\text{mod } 3)\}$
> $F_j = \{b_{(j,k)} \text{ and } c_{(j,k)} \text{ for all } k \equiv 1 \ (\text{mod } 3)\}$
> $G_j = \{b_{(j,k)} \text{ and } c_{(j,k)} \text{ for all } k \equiv 2 \ (\text{mod } 3)\}$
> $H_j = \{b_{(j,k)} \text{ and } c_{(j,k)} \text{ for all } k \equiv 0 \ (\text{mod } 3)\}$

These sets make it easier to describe which vertices are added to A when split preparing and will aid in the analysis of the critical cells. We begin with Case 1 (see Figure 9).
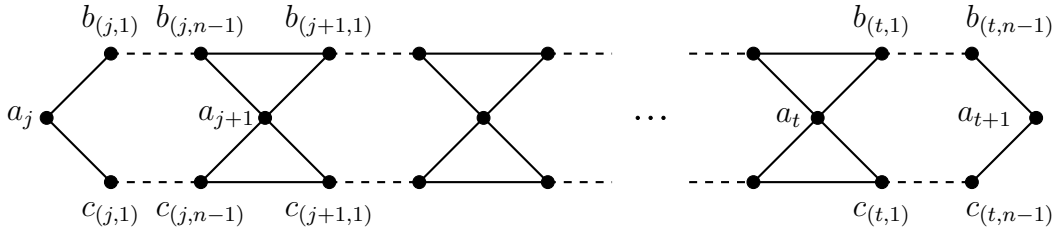
Case 1 $(\deg(a_j) = 2)$:

FIGURE 9. $G \setminus (A \cup B)$ in Case 1

<u>Left child</u>: The left child of $\Sigma(A, B)$ is $\Sigma(A, B \cup \{a_j\})$. Since $b_{(j,1)}$ and $c_{(j,1)}$ are pivots we add $b_{(j,2)}$ and $c_{(j,2)}$ to A and the neighbors of $b_{(j,2)}$ and $c_{(j,2)}$ to B. Continuing to split prepare, we add the remaining vertices of G_j to A and $N(G_j)$ to B.

- If $n \equiv 2 \pmod 3$, the largest k for which $\{b_{j,k}, c_{j,k}\} \subseteq G_j$ is $n-3$ and the last vertices added to B are $b_{j,n-2}, c_{j,n-2}$. When $j = t$, $b_{(j,n-1)}$ and $c_{(j,n-1)}$ are pivots with a_{t+1} as the associated matching vertex, so we add a_{t+1} to A and produce a critical cell. When $j \neq t$, we go to Case 2 after increasing j by one.
- If $n \equiv 1 \pmod 3$, the largest k for which $\{b_{j,k}, c_{j,k}\} \subseteq G_j$ is $n-2$ and the last vertices added to B are $b_{j,n-1}, c_{j,n-1}$. When $j = t$, a_{t+1} has no neighbors in $G \setminus (A \cup B)$, so we do not get a critical cell. When $j \neq t$, we go to Case 1 after increasing j by one.
- If $n \equiv 0 \pmod 3$, the largest k for which $\{b_{j,k}, c_{j,k}\} \subseteq G_j$ is $n-1$. When $j = t$, a_{t+1} is added to B and we have a critical cell. When $j \neq t$, unlike in the other cases, there are more pivots before we reach a split ready leaf. In this case, a_{j+1}, $b_{j+1,1}$, and $c_{j+1,1}$ are all added to B, and the situation is analogous to the right child when a_{j+1} is used as a splitting vertex except a_{j+1} is in B rather than A. In particular, instead of adding E_{j+1} to A, we add H_{j+1} and then go to Case 2 after increasing j by one.

<u>Right child</u>: The right child of $\Sigma(A, B)$ is $\Sigma(A \cup \{a_j\}, B \cup N(a_j))$. We have a situation similar to the left child, but shifted by one. We add E_j to A and $N(E_j)$ to B.
- If $n \equiv 2 \pmod 3$, the largest k for which $\{b_{j,k}, c_{j,k}\} \subseteq E_j$ is $n-2$. As in the $n \equiv 1 \pmod 3$ case for the left child, when $j = t$, a_{t+1} has no neighbors in $G \setminus (A \cup B)$, so we do not get a critical cell. When $j \neq t$, we go to Case 1 after increasing j by one.
- If $n \equiv 1 \pmod 3$, the largest k for which $\{b_{j,k}, c_{j,k}\} \subseteq E_j$ is $n-1$. As in the $n \equiv 0 \pmod 3$ case for the left child, when $j = t$, a_{t+1} is added to B and we have a critical cell. When $j \neq t$, $a_{j+1,1}, b_{j+1,1}$ and $c_{j+1,1}$ are all added to B, so there are more pivots before we reach a split ready leaf. Continuing to split prepare, we add H_{j+1} to A and $N(H_{j+1})$ to B. Then we add H_{j+2} to A and $N(H_{j+2})$ to B. This continues until we add H_t to A and $N(H_t)$ to B.
- If $n \equiv 0 \pmod 3$, the largest k for which $\{b_{j,k}, c_{j,k}\} \subseteq E_j$ is $n-3$ (unless $n = 3$, in which case $E_j = \{a_j\}$). As in the $n \equiv 2 \pmod 3$ case for the left child, when $j = t$, $b_{(j,n-1)}$ and $c_{(j,n-1)}$ are pivots with a_{t+1} as the associated matching vertex, so we add a_{t+1} to A and produce a critical cell. When $j \neq t$, we go to Case 2 after increasing j by one.
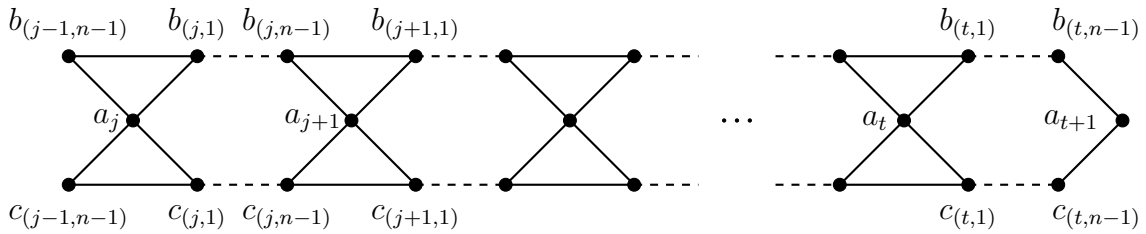
Case 2 $(\deg(a_j) = 4)$:

FIGURE 10. $G \setminus (A \cup B)$ in Case 2

Left child: The left child of $\Sigma(A, B)$ is $\Sigma(A, B \cup \{a_j\})$. Since $b_{(j-1,n-1)}$ and $c_{(j-1,n-1)}$ are pivots we add $b_{(j,1)}$ and $c_{(j,1)}$ to A and the neighbors of $b_{(j,1)}$ and $c_{(j,1)}$ to B. Continuing to split prepare, we add the remaining vertices of F_j to A and $N(F_j)$ to B.

- If $n \equiv 2 \pmod 3$ the largest k for which $\{b_{j,k}, c_{j,k}\} \subseteq F_j$ is $n - 1$. When $j = t$, a_{t+1} is added to B and we have a critical cell. When $j \neq t$, $a_{j+1,1}, b_{j+1,1}$ and $c_{j+1,1}$ are all added to B, so there are more pivots before we reach a split ready leaf. Continuing to split prepare, we add H_{j+1} to A and $N(H_{j+1})$ to B and then go to Case 1 after increasing j by one.
- If $n \equiv 1 \pmod 3$ the largest k for which $\{b_{j,k}, c_{j,k}\} \subseteq F_j$ is $n - 3$. When $j = t$, $b_{(j,n-1)}$ and $c_{(j,n-1)}$ are pivots with a_{t+1} as the associated matching vertex, so we add a_{t+1} to A and produce a critical cell. When $j \neq t$, we go to Case 2 after increasing j by one.
- If $n \equiv 0 \pmod 3$ the largest k for which $\{b_{j,k}, c_{j,k}\} \subseteq F_j$ is $n - 2$. When $j = t$, a_{t+1} has no neighbors in $G \setminus (A \cup B)$, so we do not get a critical cell. When $j \neq t$, we go to Case 1 after increasing j by one.

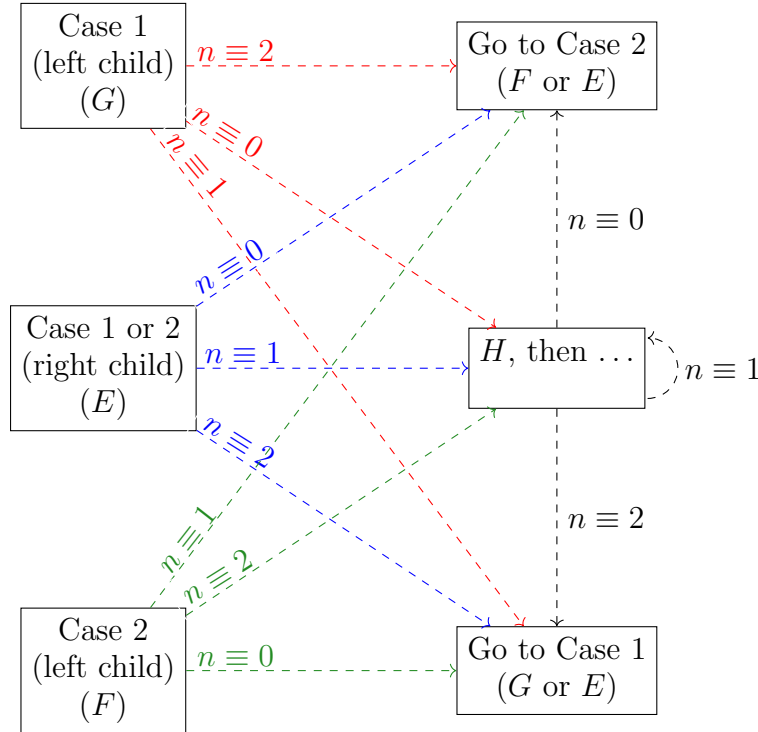Right child: The right child in Case 2 is exactly the same as the right child in Case 1.

FIGURE 11. In the analysis in the proof of Theorem 4.1, for any leaf $\Sigma(A, B)$ we represent A as a string of t letters E, F, G, and H. The chart above aids in determining which strings are possible.

Analysis: We will now determine the minimum and maximum number of vertices in the critical cells obtained from applying the Matching Tree Algorithm with our choice of splitting vertices.

By our algorithm, for any leaf $\Sigma(A, B)$ of the matching tree, $A = X_1 \cup X_2 \cup \cdots \cup X_t$ or $A = X_1 \cup X_2 \cup \cdots \cup X_t \cup \{a_{t+1}\}$ where each X_i is either E_i, F_i, G_i, or H_i. For ease of notation, we will omit the subscripts as well as a_{t+1} and represent A as a string of length t letters E, F, G, and H. For example, if $A = E_1 \cup F_2 \cup E_3 \cup \{a_{t+1}\}$, we represent it by EFE, and we say that "A begins with E," "E is followed by F," and so on. Whether or not $a_{t+1} \in A$ depends on the final letter of the string.

We use the casework above to determine which of these strings correspond to critical cells. Much of the information below is also presented in Figure 11.

If $n \equiv 0 \bmod 3$:

- A must begin with E or G, since we begin in Case 1.
- E adds $\frac{2n}{3} - 1$ vertices and is followed by E or F.
- F adds $\frac{2n}{3}$ vertices and is followed by E or G.
- G adds $\frac{2n}{3}$ vertices and is followed by H.
- H adds $\frac{2n}{3} - 2$ vertices and is followed by E or F.
- A must end with E, G, or H. We cannot end in F by the left child of Case 2.
- If A ends with E or H, add one vertex (for a_{t+1}).

By these observations, the smallest critical cells occur when A contains $\frac{2nt}{3} - t + 1$ vertices. To see this, note that while H adds the smallest number of vertices, it must be preceded by G, so the substring GH adds the same number of vertices as EE, namely $\frac{4n}{3} - 2$. Additionally, regardless of whether we end with E, G, or H, the final two letter substring adds $\frac{4n}{3} - 2$ vertices to A because of a_{j+1}. Therefore, the smallest critical cells have $\frac{2nt}{3} - t + 1$ elements and occur when A doesn't include any F's (for example, when A is a string of E's). Thus, $d^{min} = \frac{2nt}{3} - t$.

The largest critical cells occur when A contains a maximum number of F's. When t is odd, the largest critical cells occur when A is the string $EFEF \cdots FE$. When t is even, the largest critical cells occur when A is the same string but with one additional E. Therefore in the largest critical cells, A contains $\frac{2nt}{3} - \lfloor \frac{t}{2} \rfloor$ vertices. Thus, $d^{max} = \frac{2nt}{3} - \lfloor \frac{t}{2} \rfloor - 1$.

If $n \equiv 1 \bmod 3$:

- A must begin with E or G.
- E adds $\frac{2n+1}{3}$ vertices and is followed by H.
- F adds $\frac{2n+1}{3} - 1$ vertices and is followed by E or F.
- G adds $\frac{2n+1}{3} - 1$ vertices and is followed by E or G.
- H adds $\frac{2n+1}{3} - 1$ vertices and is followed by H.
- A must end with E, F or H. We cannot end in G by the left child of Case 1.
- If A ends with F, add one vertex (for a_{t+1}).

By these observations, it is impossible for A to include an F and A always contains exactly one E. Every critical cell has $\frac{2nt+t}{3} - t + 1$ elements. Thus $d^{\min} = d^{\max} = \frac{2nt+t}{3} - t$.

If $n \equiv 2 \bmod 3$:

- A must begin with E or G.

- E adds $\frac{2n-1}{3}$ vertices and is followed by E or G.
- F adds $\frac{2n-1}{3} + 1$ vertices and is followed by H.
- G adds $\frac{2n-1}{3} - 1$ vertices and is followed by E or F.
- H adds $\frac{2n-1}{3} - 1$ vertices and is followed by E or G.
- A must end with F or G. We cannot end in E by the right child of Case 1 or Case 2 or H by the left child of Case 2.
- If A ends with G, add one vertex (for a_{t+1}).

Since G and H add the smallest number of vertices, but H must be preceded by F, the smallest critical cells occur when A contains the maximum number of G's possible. When t is odd, the smallest critical cells occur when A is the string $GEGEG \cdots EG$. When t is even, the smallest critical cells occur when A is the string $EGEG \cdots EG$. Therefore the smallest critical cells have $\frac{2nt-t}{3} - \lfloor \frac{t+1}{2} \rfloor + 1$ elements and so $d^{\min} = \frac{2nt-t}{3} - \lfloor \frac{t+1}{2} \rfloor$.

The largest critical cells have $\frac{2nt-t}{3}$ elements. Note that while F adds the largest number of vertices, it must be followed by H and preceded by G, and the substring GFH adds fewer vertices than EEE. So the largest critical cells occur when A is the string $EEE \cdots EGF$ or $EEE \cdots EG$. In both cases, A has $\frac{2nt-t}{3}$ vertices so $d^{\max} = \frac{2nt-t}{3} - 1$.

$\square$

Example 4.2. Example 2.5 gives an application of Theorem 4.1 in the case where $n = 3$ and $t = 2$. In this example, the matching tree has two nonempty leaf nodes,

$$\Sigma(\{1, 6, 11\}, \{2, 3, 4, 5, 7, 8, 9, 10\}) \text{ and } \Sigma(\{4, 5, 11\}, \{1, 2, 3, 6, 7, 8, 9, 10\}).$$

Thus the two possibilities for A are $\{1, 6, 11\}$, represented by the string EE, and $\{4, 5, 11\}$, represented by the string GH. Both critical cells have size two, consistent with the fact that $d^{\max} = \frac{2(3)(2)}{3} - 2 = d^{\min}$.

Corollary 4.3. *When $n \equiv 1 \pmod 3$ and $t \geq 2$, the matching complex of t $2n$-gons is homotopy equivalent to a wedge of t spheres of dimension $\frac{2nt+t}{3} - t$.*

Proof. When $n \equiv 1 \pmod 3$ in Theorem 4.1, $d^{\max} = d^{\min} = \frac{2nt+t}{3} - t$. It follows from Theorem 2.2 that the homotopy type is a wedge of spheres. Recall from the proof of Theorem 4.1 that A can be thought of as a string of letters of length t. Furthermore, by the analysis in the $n \equiv 1$ case, there must be exactly one E in this string, which is preceded by G's and followed by H's. Since the number of critical cells is equal to the number of possible strings of length t of this form, there are t critical cells. $\square$

When $n = 3$ in Figure 8 we have a $1 \times 1 \times t$ honeycomb graph. Therefore Theorem 4.1 provides partial results for the honeycomb question that arises in [21].

Corollary 4.4. *The matching complex of a $1 \times 1 \times t$ honeycomb graph is at least $(t-1)$-connected.*

Proof. When $t \geq 2$, this follows immediately from the $n = 3$ case of Theorem 4.1. When $t = 1$, a $1 \times 1 \times t$ honeycomb graph is the cycle C_6, and $M(C_6) \simeq S^1 \vee S^1$ [24, Proposition 4.6]. $\square$

Theorem 4.1 provides a particular family of graphs that sharpen previous connectivity bounds due to Barmak [2] and Engström [13] when applied to lines of $2n$-gons. In these papers, the authors independently explored the connectivity of the independence complexes

of claw-free graphs. The *claw graph* is the complete bipartite graph $K_{1,3}$. A graph is *claw-free* if there are no induced subgraphs which are claw graphs.

As the matching complex of a graph is the independence complex of the line graph, and all line graphs are claw-free, Barmak's and Engström's results can be used to obtain connectivity bounds for matching complexes. Barmak and Engström's results apply to a much larger class of graphs. However, for the specific families of graphs we consider in Theorem 4.1, our bounds are sharper than the bounds provided by Barmak [2, Theorem 5.5] and Engström [13, Theorem 3.2].

Engström shows that for a claw-free graph G with n vertices and maximum degree d, $\text{Ind}(G)$ is $\lfloor \frac{2n-1}{3d+2} - 1 \rfloor$-connected [13, Theorem 3.2]. The line graph of t $2n$-gons has $(2n-1)t+1$ vertices and maximum degree 4, so Engström's result implies that $\text{Ind}(L(G)) = M(G)$ is $(\lfloor \frac{4tn-2t+1}{14} \rfloor - 1)$-connected which is less than or equal to $d^{\min}$ for all $n \geq 0$.

In [2], Barmak provide a connectivity bound based off the dimension of the complex. The result states if $L(G)$ is claw-free, then $M(G)$ is $\frac{\dim(M(G))-2}{2}$-connected [2, Theorem 5.5]. The dimension of the matching complex of t $2n$-gons is $(n-1)t+1$, which provides a connectivity bound of $\frac{tn-t-1}{2}$. While Barmak's result provides a sharper connectivity bound than Engström's for large values of n, the results presented here are sharper still for all $n \geq 1$.

We will show in Theorem 4.8 that the $2 \times 1 \times t$ honeycomb is $(2t-1)$-connected. Again, when we compare our results to those of Barmak and Engström, we see that the results presented here are sharper for these honeycombs. We start with a weak connectivity bound for any $r \times s \times t$ honeycomb graph based on the values of r, s, and t. Notice that a honeycomb and its line graph have $r + s - 1$ rows of hexagons.

Remark 4.5. The number of hexagons in the ith row from the top of an $r \times s \times t$ honeycomb graph (or line graph) is $\rho(i)$, where

$$\rho(i) = \begin{cases} t+i-1 & \text{if } 1 \leq i \leq \min(r,s) \\ t+\min(r,s)-1 & \text{if } \min(r,s) < i \leq \max(r,s) \\ t+r+s-1-i & \text{if } \max(r,s) < i \leq r+s-1 \end{cases}$$
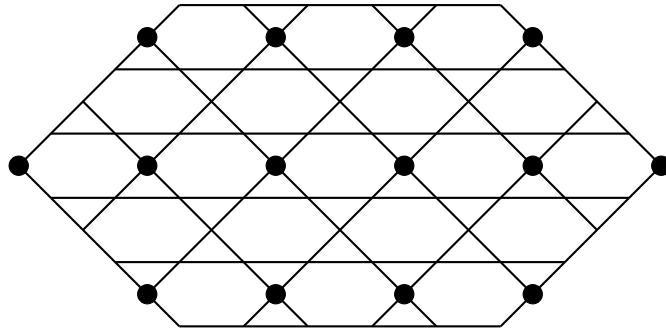

FIGURE 12. The line graph of a $3 \times 3 \times 3$ honeycomb

Proposition 4.6. *The matching complex of an $r \times s \times t$ honeycomb graph G is at least k-connected, where*

$$k = t \left\lceil \frac{r+s-1}{2} \right\rceil + \left\lceil \frac{\max(r,s)\min(r,s)}{2} \right\rceil - 2.$$

Proof. Consider the subset $X \subset V(G)$ consisting of the center vertices of each hexagon in every ith row for all $i \in \{1,3,5,\ldots,r+s-1\}$ (see Figure 12). Each row contributes one more vertex than the number of hexagons in the row. We see that $|X| = \sum_{i=1}^{\lceil \frac{r+s-1}{2} \rceil} (\rho(2i-1)+1)$, where $\rho(i)$ is defined in Remark 4.5. Since the neighbors of each vertex are disjoint, we can apply Lemma 2.8 to conclude that all critical cells have at least $\sum_{i=1}^{\lceil \frac{r+s-1}{2} \rceil} (\rho(2i-1)+1)$ elements. We claim that

$$\sum_{i=1}^{\lceil \frac{r+s-1}{2} \rceil} (\rho(2i-1)+1) = t \left\lceil \frac{r+s-1}{2} \right\rceil + \left\lceil \frac{\max(r,s)\min(r,s)}{2} \right\rceil$$

We will prove this when r and s are odd. The general case is similar. By the definition of ρ,

$$\sum_{i=1}^{\lceil \frac{r+s-1}{2} \rceil} (\rho(2i-1)+1)$$

$$= \sum_{i=1}^{\lceil \frac{r+s-1}{2} \rceil} t + \sum_{i=1}^{\frac{\min(r,s)+1}{2}} (2i-1) + \sum_{i=\frac{\min(r,s)+1}{2}+1}^{\frac{\max(r,s)+1}{2}} \min(r,s) + \sum_{i=\frac{\max(r,s)+1}{2}+1}^{\lceil \frac{r+s-1}{2} \rceil} (r+s-2i+1).$$

Since $\sum_{i=\frac{\max(r,s)+1}{2}+1}^{\lceil \frac{r+s-1}{2} \rceil} (r+s-2i+1) = \sum_{i=1}^{\frac{\min(r,s)-1}{2}} (\min(r,s)-2i)$, we see that

$$\sum_{i=1}^{\lceil \frac{r+s-1}{2} \rceil} (\rho(2i-1)+1) = \sum_{i=1}^{\lceil \frac{r+s-1}{2} \rceil} t + \left(\sum_{i=1}^{\frac{\max(r,s)+1}{2}} \min(r,s) \right) - \frac{\min(r,s)-1}{2}$$

$$= t \left\lceil \frac{r+s-1}{2} \right\rceil + \left\lceil \frac{\max(r,s)\min(r,s)}{2} \right\rceil$$

The connectivity bound follows. $\qquad\qquad\square$

Proposition 4.6 gives another proof of Corollary 4.4. However, for a $2 \times 1 \times t$ honeycomb graph, we can greatly improve the connectivity bound through casework. Furthermore, this method will give us both upper and lower bounds for the sizes of the critical cells.

The following lemma describes the outcome to applying the Matching Tree Algorithm to a configuration that frequently occurs in the proof of Theorem 4.8.

Lemma 4.7. *Let $\Sigma(A, B)$ be a split ready leaf associated to the configuration with a hexagon and a triangle that share an edge.*

19

Then, after completing the Matching Tree Algorithm, the two leaf nodes $\Sigma(\tilde{A}, \tilde{B})$, $\Sigma(\hat{A}, \hat{B})$ with lowest common ancestor $\Sigma(A, B)$ have $|\tilde{A}| = |\hat{A}| = |A| + 2$.

Proof. Choose the indicated vertex of the hexagon as our next splitting vertex, as pictured to the right[1]. Then splitting produces two leaves, $\Sigma(A, B \cup \{v\})$ and $\Sigma(A \cup \{v\}, B \cup N(v))$.

When split preparing the left child $\Sigma(A, B \cup \{v\})$ we add two matching vertices to A. When split preparing the right child $\Sigma(A \cup \{v\}, B \cup N(v))$, we add one matching vertex to $A \cup \{v\}$. Thus, the two children of $\Sigma(A, B)$ have critical cells with $|A| + 2$ elements.

$\square$
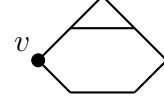
Theorem 4.8. *Let $t \geq 1$ and $n > 2$. Define*

$$d^{\min} = 2t$$

and

$$d^{\max} = \frac{7t}{3} + 1$$

The matching complex of a $2 \times 1 \times t$ honeycomb graph is homotopy equivalent to a space with no d-dimensional cells, where $0 < d < d^{\min}$ and $d \geq d^{\max}$. Further, the connectivity is at least $d^{min} - 1$.

Proof. A $2 \times 1 \times t$ honeycomb is made up of two rows of t hexagons with the line graph shown in Figures 13 and 14.

The proof of this theorem is similar to the proof of Theorem 4.1. We will again use the Matching Tree Algorithm with specific choices of splitting vertices. However, unlike in Theorem 4.1, at each step the choice of the next splitting vertex depends on the current configuration. We apply the following algorithm:

For each split ready leaf node $\Sigma(A, B)$:

> Step 1: Choose the appropriate splitting vertex v depending on the current configuration. This produces two leaves, $\Sigma(A, B \cup \{v\})$ and $\Sigma(A \cup \{v\}, B \cup N(v))$.
> Step 2: Split prepare each leaf.

At Step 1 of this algorithm, there will be six possible configurations distinguished by the leftmost part of the graph up to vertical reflection, as seen in Figure 13 and Figures 15 – 19. For each of these cases, we mark the splitting vertex in bold. Note that our choices of splitting vertices is somewhat arbitrary. They are intended to minimize casework, but it is possible that our choices could be further optimized.

Let $\mathrm{T_{hex}} := \mathrm{T_{hex}}(\Sigma(A, B))$ be the number of complete hexagons in $G \setminus (A \cup B)$. Note that $\mathrm{T_{hex}}(\Sigma(\emptyset, \emptyset)) = 2t$ and $\mathrm{T_{hex}}(\Sigma(A, B)) = 0$ when $\Sigma(A, B)$ corresponds to a critical cell.

As we move down our matching tree, we add vertices to the left set of the matching tree nodes. When $\Sigma(A', B')$ is a descendant of $\Sigma(A, B)$ we will abuse notation by saying that $|A|$ "increases" by $|A'| - |A|$ as we go from $\Sigma(A, B)$ to $\Sigma(A', B')$. As we proceed through the algorithm, we will keep track of $|A|$, which will increase as we move down the matching tree and $\mathrm{T_{hex}}$, which will decrease as we move down the matching tree. We calculate d^{min} and d^{max} by observing the relationship between the changes to $|A|$ and $\mathrm{T_{hex}}$.

Case 1:

---

[1]For this configuration, the choice of splitting vertex does not affect the size or quantity of critical cells, but this is not true for all configurations.
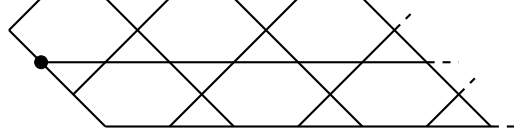
FIGURE 13. Case 1

- For the left child $(\Sigma(A, B \cup \{v\}))$:
    - If $T_{hex} = 2$, we have the configuration pictured right. We add one matching vertex to A when split preparing, and the next configuration is one hexagon and a triangle that share an edge. By Lemma 4.7, we get two critical cells. For each of the cells, $|A|$ increases by 3 while T_{hex} decreases by 2.
    - If $T_{hex} \geq 3$, we add one matching vertex to A, decrease T_{hex} by one, and repeat Case 1, as a vertical reflection. The argument is analogous by symmetry. From now on, we will take these vertical symmetries for granted without further comment.
- For the right child $(\Sigma(A \cup \{v\}, B \cup N(v)))$:
    - If $T_{hex} \leq 5$, we get no critical cell.
    - If $T_{hex} = 6$, we add five vertices to A when split preparing, including v (see Figure 14). We are left with one hexagon with two attached triangles and we choose our next splitting vertex to be any of the vertices on both the hexagon and a triangle. Then, we get one critical cell, adding two more vertices to A: either two matching vertices or one splitting and one matching vertex. Thus, for each critical cell, $|A|$ increases by 7 while T_{hex} decreases by 6.
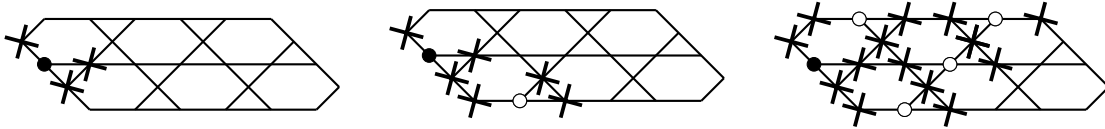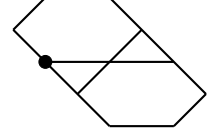   - If $T_{hex} > 6$, we add five vertices to A including v, decrease T_{hex} by five, and go to Case 2.

FIGURE 14. Case 1 for $T_{hex} = 6$: The vertices in A are represented with a circle, where an open circle represents a matching vertex. The vertices in B are represented with an "X." The leftmost image shows the splitting vertex in A and its neighborhood in B. Continuing to split prepare, we see there are two possible matching vertices. The middle picture shows the result of choosing one of them. We continue this process until there are no more matching vertices, shown in the rightmost image. We are left with a hexagon with two attached triangles.

Case 2:

- For the left child $(\Sigma(A, B \cup \{v\}))$:
    - We do not add anything to A or change T_{hex}. Go back to Case 1.
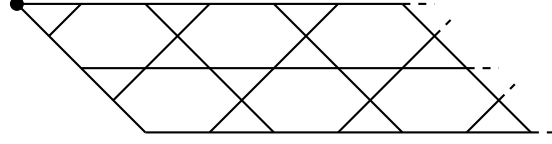- For the right child $(\Sigma(A \cup \{v\}, B \cup N(v)))$:

21

FIGURE 15. Case 2

- If $T_{hex} = 2$, we get a critical cell after adding four vertices to A, including v.
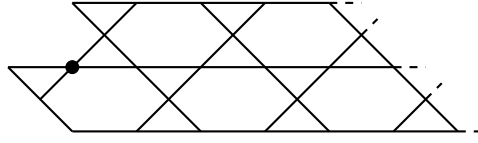- If $T_{hex} \geq 3$, we only add v to A, decrease T_{hex} by one, then go to Case 3.

Case 3:

FIGURE 16. Case 3

- For the left child ($\Sigma(A, B \cup \{v\})$):
  - If $T_{hex} = 2$, we get a critical cell after adding four matching vertices to A.
  - If $T_{hex} \geq 3$, we add one matching vertex to A, decrease T_{hex} by one, and go to Case 4.
- For the right child ($\Sigma(A \cup \{v\}, B \cup N(v))$):
  - If $T_{hex} = 2$, we get a critical cell after adding four vertices to A, including v.
  - If $T_{hex} = 3$, we get a critical cell after adding five vertices to A, including v.
  - If $T_{hex} = 4$, we get a critical cell after adding six vertices to A, including v.
  - If $T_{hex} \geq 5$, we add three vertices to A, including v, and decrease T_{hex} by three before repeating Case 3.

Case 4:
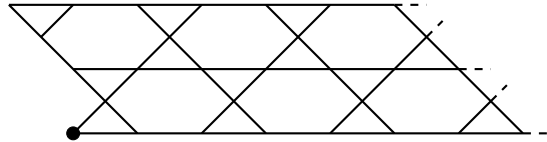

FIGURE 17. Case 4

- For the left child ($\Sigma(A, B \cup \{v\})$):
  - We do not add anything to A or change T_{hex}. Go back to Case 2.
- For the right child ($\Sigma(A \cup \{v\}, B \cup N(v))$):
  - If $T_{hex} = 2$, we add two vertices to A including v, and are left with a hexagon and a triangle that share an edge. By Lemma 4.7, we get two critical cells. For each of the cells, $|A|$ increases by 4.

22

– If $T_{hex} = 3$, we add three vertices to A including v, and are left with a hexagon and a triangle that share an edge. By Lemma 4.7, we get two critical cells. For each of the cells, $|A|$ increases by 5.
– If $T_{hex} \geq 4$, we only add v to A, decrease T_{hex} by one, then go to Case 5.

Case 5:

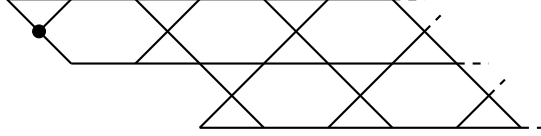
FIGURE 18. Case 5

- For the left child $(\Sigma(A, B \cup \{v\}))$:
  – If $T_{hex} = 3$, we add three matching vertices to A, and are left with a hexagon and a triangle that share an edge. By Lemma 4.7, we get two critical cells. For each of the cells, $|A|$ increases by 5.
  – If $T_{hex} = 4$, we add four matching vertices to A, and are left with a hexagon and a triangle that share an edge. By Lemma 4.7, we get two critical cells. For each of the cells, $|A|$ increases by 6.
  – If $T_{hex} = 5$, we add five matching vertices to A, and are left with a hexagon and a triangle that share an edge. By Lemma 4.7, we get two critical cells. For each of the cells, $|A|$ increases by 7.
  – If $T_{hex} \geq 6$, we add three matching vertices to A and decrease T_{hex} by 3, then repeat Case 5.
- For the right child $(\Sigma(A \cup \{v\}, B \cup N(v)))$:
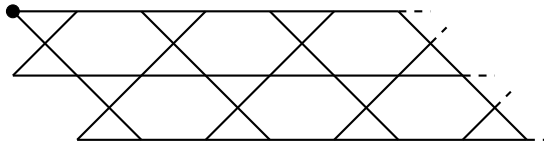 – We only add v to A, decrease T_{hex} by one, and go to Case 6.

Case 6:

FIGURE 19. Case 6

- For the left child $(\Sigma(A, B \cup \{v\}))$:
  – We do not add anything to A or change T_{hex}. Go back to Case 3.
- For the right child $(\Sigma(A \cup \{v\}, B \cup N(v)))$:
  – If $T_{hex} = 2$, we get no critical cells.
  – If $T_{hex} \geq 3$, we add three vertices to A, including v, decrease T_{hex} by two, then go back to Case 2.
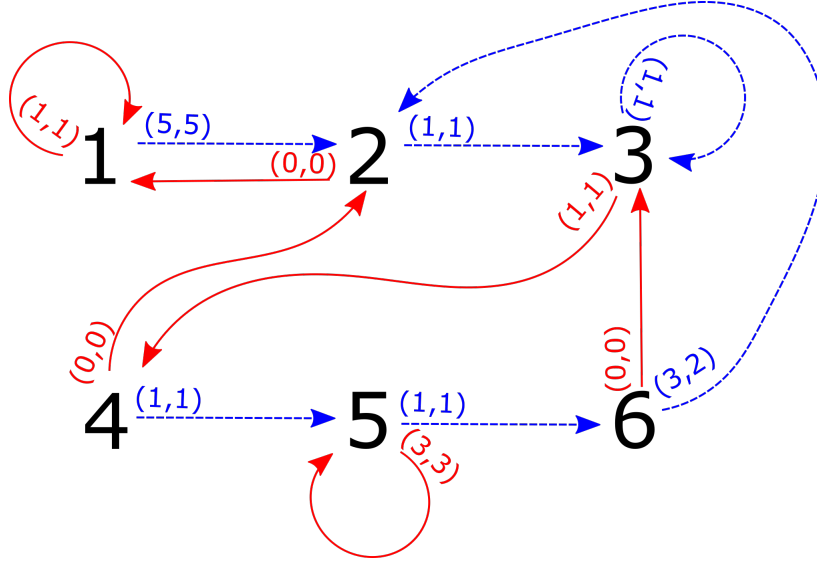
23

FIGURE 20. In the proof of Theorem 4.8, there are six possible configurations, labeled 1 through 6 above. Choosing the appropriate splitting vertex produces two leaves: a left child and a right child. After split preparing each child, we arrive at new configurations. The blue dashed lines are the right children while the red solid lines are the left children. The pair of values at each line are the increase to $|A|$ and the decrease to $\mathrm{T}_{\mathrm{hex}}$, respectively, from one configuration to the next. Note that the only time that they are not equal is when we go from 6 to 2. Here, we add 3 vertices to A but only remove 2 hexagons.

Analysis: Figure 20 will aid in the analysis. Observe that in every case, $|A|$ increases at least as much as $\mathrm{T}_{\mathrm{hex}}$ decreases. Furthermore, whenever a critical cell is produced, $|A|$ increases strictly more than $\mathrm{T}_{\mathrm{hex}}$ decreases. Since $\mathrm{T}_{\mathrm{hex}} = 2t$ at the start, the size of every critical cell is at least $2t + 1$ and it follows that $d^{\min} = 2t$.

To find $d^{\max}$, we observe that we only increase $|A|$ more than we decrease $\mathrm{T}_{\mathrm{hex}}$ without creating a critical cell in the right child of Case 6. The unique cycle containing this child is also made up of the right child of Case 2, the left child of Case 3, the right child of Case 4, and the right child of Case 5. Going once through this cycle increases $|A|$ by 7 and decreases $\mathrm{T}_{\mathrm{hex}}$ by 6. It follows that if we start from Case 2 and proceed through several steps of the algorithm without creating a critical cell, the most we can increase $|A|$ is $\frac{7}{6}$ of the amount we decrease $\mathrm{T}_{\mathrm{hex}}$. To get from Case 1 to Case 2, we have to first increase $|A|$ by 5 and decrease $\mathrm{T}_{\mathrm{hex}}$ by 5. This means that if we start from Case 1 and proceed through several steps of the algorithm without creating a critical cell, we increase $|A|$ by strictly less than $\frac{7}{6}$ of the amount we decrease $\mathrm{T}_{\mathrm{hex}}$. When we do create a critical cell, the difference between the amount we increase $|A|$ and the amount we decrease $\mathrm{T}_{\mathrm{hex}}$ is at most 2. Thus, the largest critical cells must be smaller than $\frac{7}{6}(2t) + 2 = \frac{7t}{3} + 2$, and $d^{\max} = \frac{7t}{3} + 1$. $\square$

Remark 4.9. Corollary 4.4 and Theorem 4.8 show that for $1 \times 1 \times t$ and $2 \times 1 \times t$ honeycomb graphs, the connectivity of the matching complex is at least one less than the number of hexagons in the graph. However, this is not true in general. Using homology tools in Sage,

we found that H_9 of the matching complex of a $3 \times 2 \times 1$ honeycomb is $\mathbb{Z} \times \mathbb{Z}$. Because H_9 is nontrivial, the honeycomb is at most 8-connected, although it contains 10 hexagons.

5. Matching Complexes of Trees

In this section, we use the tools from Section 2.3 to determine the explicit homotopy type of matching complexes of particular types of trees. Marietti and Testa proved the following:

Theorem 5.1. [27, Theorem 4.13] *Let G be a forest. Then $M(G)$ is either contractible or homotopy equivalent to a wedge of spheres.*

We build on this result by determining the explicit homotopy type for caterpillar graphs.

5.1. Matching Complexes of Caterpillar Graphs.
A *caterpillar graph* is a tree in which every vertex is on a central path or only one edge away from the path. By Theorem 5.1, we know that the matching complex of caterpillar graphs is a wedge summand of spheres (or contractible). In [27], Marietta and Testa note that one can compute the number of spheres in each dimension recursively using [27, Proposition 3.3]. We found that in special cases nice formulas arise.

A table giving the homotopy type of small caterpillar graphs can be found in the Appendix. In general, the number of spheres in each dimension is complex, so we first present a special case to illustrate the main ideas.

Definition 5.2. A *perfect m-caterpillar of length n* is a caterpillar graph with m legs at each vertex on the central path of n vertices (see Figure 21).
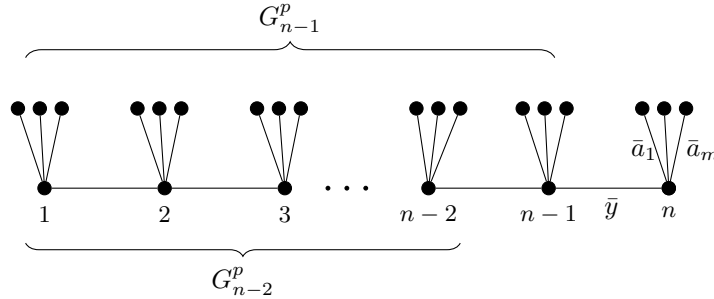

FIGURE 21. A perfect m-caterpillar of length n.

Theorem 5.3. *For $m \geq 2$, let G_n^p be a perfect m-caterpillar graph of length $n \geq 1$. Then the homotopy type of $M(G_n^p)$ is given by:*
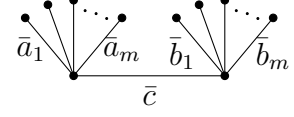
$$
(1) \qquad M(G_n^p) \simeq \begin{cases} \displaystyle\bigvee_{t=0}^{k} \bigvee_{\alpha_t} S^{k-1+t} & \text{if } n = 2k \\ \displaystyle\bigvee_{t=0}^{k} \bigvee_{\beta_t} S^{k+t} & \text{if } n = 2k+1 \end{cases}
$$

where $\alpha_t = \binom{k+t}{k-t}(m-1)^{2t}$ and $\beta_t = \binom{k+1+t}{k-t}(m-1)^{2t+1}$.

25

Proof. We proceed by induction. Consider the cases G_1^p and G_2^p. $M(G_1^p)$ consists of a discrete set of m points. Therefore, $M(G_1^p) \simeq \bigvee_{m-1} S^0$, which satisfies (1) when $n = 1$. Now, consider G_2^p with edges labeled as shown to the right. Then $M(G_2^p)$ is $K_{m,m} \bigsqcup c$, where $K_{m,m}$ denotes a complete bipartite graph. Since $K_{m,m} \simeq \bigvee_{(m-1)^2} S^1$ we see that $M(G_2^p) \simeq S^0 \vee \left[\bigvee_{(m-1)^2} S^1 \right]$, which satisfies (1) when $n = 2$.

Suppose now that the theorem holds for $G_1^p, G_2^p, \ldots, G_{2(k-1)+1}^p, G_{2k}^p$ $(k \geq 1)$. We prove (1) holds for G_{2k+1}^p and G_{2k+2}^p.

Label the edges of G_n^p as shown in Figure 21 and apply Lemma 2.14. Since $\text{del}_G(\overline{a}_1) = G_{n-1}^p$ and $\text{del}_G(\overline{y}) = G_{n-2}^p$ when $n \geq 3$ we have

$$M(G_n^p) \simeq \left[\bigvee_{m-1} S(M(G_{n-1}^p)) \right] \vee S(M(G_{n-2}^p)).$$

Using Remark 2.11 and the induction hypothesis, when $n = 2k + 1$ we obtain:

$$
\begin{aligned}
M(G_{2k+1}^p) \quad &\simeq \quad \left[\bigvee_{m-1} S(M(G_{2k}^p)) \right] \vee S(M(G_{2(k-1)+1}^p)) \\[2mm]
&\simeq \quad \left[\bigvee_{m-1} S \left[\bigvee_{t=0}^{k} \bigvee_{\binom{k+t}{k-t}(m-1)^{2t}} S^{k-1+t} \right] \right] \vee S \left[\bigvee_{t=0}^{k-1} \bigvee_{\binom{k+t}{k-1-t}(m-1)^{2t+1}} S^{k-1+t} \right] \\[2mm]
&\simeq \quad \left[\bigvee_{t=0}^{k} \bigvee_{\binom{k+t}{k-t}(m-1)^{2t+1}} S(S^{k-1+t}) \right] \vee \left[\bigvee_{t=0}^{k-1} \bigvee_{\binom{k+t}{k-1+t}(m-1)^{2t+1}} S(S^{k-1+t}) \right] \\[2mm]
&\simeq \quad \left[\bigvee_{t=0}^{k} \bigvee_{\binom{k+t}{k-t}(m-1)^{2t+1}} S^{k+t} \right] \vee \left[\bigvee_{t=0}^{k-1} \bigvee_{\binom{k+t}{k-1+t}(m-1)^{2t+1}} S^{k+t} \right] \\[2mm]
&\cong \quad \left[\bigvee_{t=0}^{k-1} \bigvee_{(\binom{k+t}{k-t}+\binom{k+t}{k-1+t})(m-1)^{2t+1}} S^{k+t} \right] \vee \left[\bigvee_{\binom{k+k}{k-k}(m-1)^{2k+1}} S^{2k} \right] \\[2mm]
&\cong \quad \left[\bigvee_{t=0}^{k-1} \bigvee_{\binom{k+1+t}{k-t}(m-1)^{2t+1}} S^{k+t} \right] \vee \left[\bigvee_{\binom{2k}{0}(m-1)^{2k+1}} S^{2k} \right] \\[2mm]
&= \quad \bigvee_{t=0}^{k} \bigvee_{\binom{k+1+t}{k-t}(m-1)^{2t+1}} S^{k+t}.
\end{aligned}
$$

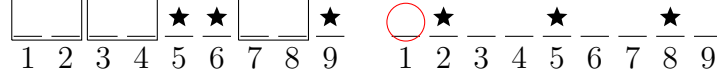The proof for G_{2k+2}^p is completely analogous.

$\square$

FIGURE 22. $(5, 6, 9) \in A_3^9$ but $(2, 5, 8) \notin A_3^9$

Notice that the number of spheres of dimension d in the homotopy type of perfect 2-caterpillars are counted by binomial coefficients.

Remark 5.4. The homotopy type of a perfect 1-caterpillar graph of length $n \geq 1$ is

(2)
$$M(G_n^p) \simeq \begin{cases} S^{k-1} & \text{if } n = 2k \\ \text{pt} & \text{if } n = 2k + 1 \end{cases}$$

The proof is the same as the proof of Theorem 5.3.

We now generalize to all caterpillar graphs with each central vertex incident to at least one leg. Table 1 contains calculations for the number of spheres in each dimension for the homotopy type of these caterpillar graphs. While this table appears more complex, the entries have a nice combinatorial interpretation.

To describe the combinatorial interpretation we define the following class of subsequences of $[n] := (1, 2, \ldots, n)$, which will enumerate the number of spheres of each dimension.

Definition 5.5. Let $n, x \in \mathbb{N}$.
$A_x^n := \{(i_1, i_2, \ldots, i_x) \subseteq [n] \mid 1 \leq i_1 < i_2 < \cdots < i_x \leq n$ and after marking the selected x positions the remaining $n - x$ positions can be covered with $\frac{n-x}{2}$ disjoint 2-blocks.$\}$

When $n - x$ is odd, $A_x^n = \emptyset$. When $n = 2k$ and $x = 0$, $A_0^{2k} = \{\emptyset\}$, so $|A_0^{2k}| = 1$.

Example 5.6. (Examples of A_x^n)
  (1) When $x = n$, $A_n^n = \{(1, 2, \ldots, n)\}$.
  (2) In Figure 22, we illustrate two subsequences of $(1, 2, \ldots, 9)$: one that is an element of A_3^9 and one that is not.

Remark 5.7. Let $a_x^n = |A_x^n|$ denote the size of A_x^n. Then when n and x have the same parity,

$$a_x^n = \binom{\frac{n+x}{2}}{\frac{n-x}{2}},$$

which can be obtained by counting the number of possible arrangements.

Definition 5.8. For any choice of n nonnegative numbers $t_1, t_2, \ldots, t_n \in \mathbb{N}$ and $x \in \mathbb{N}$ such that $n - x$ is even, define the sum

$$M_x^n = \sum_{(i_1, i_2, \ldots, i_x) \in A_x^n} t_{i_1} t_{i_2} \cdots t_{i_x}$$

Example 5.9. (Examples of M_x^n).
  (1) When $x = n$, $A_n^n = \{(1, 2, 3, \ldots, n)\}$, so $M_n^n = t_1 t_2 \cdots t_n$.
  (2) When n is odd and $x = 1$, $A_1^{2k+1} = \{(1), (3), (5), \ldots, (2k + 1)\}$, so $M_1^{2k+1} = t_1 + t_3 + t_5 + \cdots + t_{2k+1}$.
  (3) For an explicit example, consider when $n = 4$ and $x = 2$. Then, $A_2^4 = \{(1, 2), (1, 4), (3, 4)\}$ and $M_2^4 = t_1 t_2 + t_1 t_4 + t_3 t_4$.
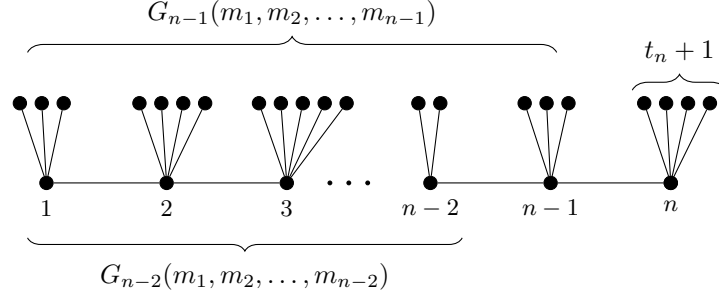
27

FIGURE 23. A caterpillar graph of length n.

Lemma 5.10. *The polynomials $M_x^n(t_1, \ldots, t_n)$ satisfy the following relations for $1 \le \ell \le k$:*

(a) $M_{2\ell+1}^{2k+1} = M_{2\ell}^{2k} t_{2k+1} + M_{2\ell+1}^{2k-1}$

(b) $M_{2\ell}^{2k+2} = M_{2\ell-1}^{2k+1} t_{2k+2} + M_{2\ell}^{2k}$

Proof. We will only prove (a) as the proof of (b) is completely analogous. By definition, $M_{2\ell+1}^{2k+1} = \sum_{(i_1, \ldots, i_{2\ell+1}) \in A_{2\ell+1}^{2k+1}} t_{i_1} t_{i_2} \cdots t_{i_{2\ell+1}}$. We partition the sequences in $A_{2\ell+1}^{2k+1}$ into two groups based on whether $i_{2\ell+1} = 2k+1$ or $i_{2\ell+1} < 2k+1$.

(1) If $i_{2\ell+1} = 2k+1$ then from the first $2k$ positions we choose 2ℓ positions that we mark so that the unmarked positions can be covered with $\frac{2k-2\ell}{2}$ disjoint 2-blocks. The terms in $M_{2\ell+1}^{2k+1}$ that correspond to these subsequences in $A_{2\ell+1}^{2k+1}$ are exactly the terms in $M_{2\ell}^{2k} t_{2k+1}$.

(2) If $i_{2\ell+1} < 2k+1$, the last position is not marked so positions $2k$ and $2k+1$ must be covered with one 2-block. We choose $2\ell + 1$ positions to mark among the first $2k - 1$ positions, respecting the rule. The sum corresponding to these subsequences is $M_{2\ell+1}^{2k-1}$.

Combining (1) and (2) proves that $M_{2\ell+1}^{2k+1} = M_{2\ell}^{2k} t_{2k+1} + M_{2\ell+1}^{2k-1}$. $\qquad\square$

Theorem 5.11. *Let $G_n = G_n(m_1, \ldots, m_n)$ be a caterpillar graph with m_i legs, $m_i \ge 1$, at each vertex i on the central path of length $n \ge 1$. Then the homotopy type of $M(G_n)$ is given by:*

$$M(G_n) \simeq \begin{cases} \bigvee_{\ell=0}^{k} \bigvee_{M_{2\ell}^{2k}} S^{k-1+\ell} & \text{if } n = 2k \\ \bigvee_{\ell=0}^{k} \bigvee_{M_{2\ell+1}^{2k+1}} S^{k+\ell} & \text{if } n = 2k+1 \end{cases}$$

where all sums M_x^n are $M_x^n(t_1, t_2, \ldots, t_n)$ with $t_i := m_i - 1$.

Proof. We proceed by induction, using G_1 and G_2 as our base cases. When $n = 1, k = 0$ and $M_1^1 = t_1$. Notice that $M(G_1) = [m_1] \simeq \bigvee_{m_1-1} S^0 = \bigvee_{t_1} S^0$ as expected. When $n = 2, k = 1$, and $M_2^2(t_1, t_2) = t_1 t_2$. The matching complex of G_2 is a 1-dimensional complex consisting of a disjoint point and a bipartite graph with the shores consisting of $t_1 + 1$ and $t_2 + 1$ vertices respectively. Therefore, $M(G_2) \simeq S^0 \vee \left[\bigvee_{t_1 t_2} S^1 \right]$.

28

Assume the theorem holds for $G_1, G_2, \ldots, G_{2(k-1)+1}, G_{2k}$. We show that it holds for G_{2k+1} and G_{2k+2} for $k \geq 1$. As in the proof of Theorem 5.3, applying Lemma 2.14 we find that

$$M(G_n) \simeq \left[\bigvee_{t_n} S(M(G_{n-1}))\right] \vee S(M(G_{n-2}))$$

for $n \geq 3$ as shown in Figure 23. Proceeding as we did in Theorem 5.3, we use the properties of suspensions of wedges of spheres from Remark 2.11 to see that:

$$
\begin{aligned}
M(G_{2k+1}) &\simeq \left[\bigvee_{t_{2k+1}} S(M(G_{2k}))\right] \vee S(M(G_{2(k-1)+1})) \\
&\simeq \left[\bigvee_{t_{2k+1}} S\left[\bigvee_{\ell=0}^{k} \bigvee_{M_{2\ell}^{2k}} S^{k-1+\ell}\right]\right] \vee S\left[\bigvee_{\ell=0}^{k-1} \bigvee_{M_{2\ell+1}^{2(k-1)+1}} S^{k-1+\ell}\right] \\
&\simeq \left[\bigvee_{t_{2k+1}} \bigvee_{\ell=0}^{k} \bigvee_{M_{2\ell}^{2k}} S(S^{k-1+\ell})\right] \vee \left[\bigvee_{\ell=0}^{k-1} \bigvee_{M_{2\ell+1}^{2(k-1)+1}} S(S^{k-1+\ell})\right] \\
&= \left[\bigvee_{\ell=0}^{k-1} \bigvee_{M_{2\ell}^{2k} t_{2k+1} + M_{2\ell+1}^{2(k-1)+1}} S^{k+\ell}\right] \vee \left[\bigvee_{M_{2k}^{2k} t_{2k+1}} S^{2k}\right]
\end{aligned}
$$

Since by Lemma 5.10, $M_{2\ell}^{2k} t_{2k+1} + M_{2\ell+1}^{2k-1} = M_{2\ell+1}^{2k+1}$, and $M_{2k}^{2k} t_{2k+1} = t_1 t_2 \cdots t_{2k} t_{2k+1} = M_{2k+1}^{2k+1}$, the statement holds for $M(G_{2k+1})$.

For $n = 2k + 2$ the argument follows similarly which proves the case for $M(G_{2k+2})$.

$\square$

Remark 5.12. There is another proof of Theorem 5.11 that uses inflated simplicial complexes and Theorem 6.2 from [5]. The main idea is to notice that the matching complex of $G_n(m_1, \ldots, m_n)$ can be considered as the m-inflation Δ_m of the matching complex $\Delta = M(G_n^p)$, where G_n^p is the perfect 1-caterpillar graph. This m-inflation provides insight into the combinatorial interpretation of the polynomials M_x^n.

5.2. **The homotopy type for general caterpillar graphs.** Thus far, we have determined the explicit homotopy type of caterpillar graphs $G_n = G_n(m_1, \ldots, m_n)$ in the case where $m_i \geq 1$ for all i. For arbitrary caterpillar graphs that may have vertices on the central path without any legs, there is no obvious formula that gives the number of spheres in each dimension. In this section, we provide a general procedure that inductively constructs the explicit homotopy type of $M(G_n(m_1, \ldots, m_n))$ where $m_i \geq 0$. More precisely, we have the following theorem.

Theorem 5.13. *Let* $G_n = G_n(m_1, \ldots, m_n)$ *be a caterpillar graph on a central path of* n *vertices such that the ith vertex is a m_i-leg, where* $n \geq 3$, $m_i \geq 0$ *and* $m_1 \geq 1$. *Let* $t_i = m_i - 1$. *Let* $A_{n,d}$ *denote the number of spheres of dimension d in the homotopy type of* $M(G_n)$. *Then*

$$A_{n+1,d} = \begin{cases} t_{n+1}A_{n,d-1} + A_{n-1,d-1} & \text{if } m_{n+1} \geq 1 \\ A_{n,d} + A_{n-1,d-1} & \text{if } m_{n+1} = 0 \text{ and } m_n \geq 1 \, . \\ A_{n-2,d-1} & \text{if } m_{n+1} = m_n = 0 \end{cases}$$

Proof. There are three cases to consider:

Case 1: $(m_{n+1} \geq 1$ and $m_n \geq 0$ for all $n)$
   Under these assumptions, we have as a direct consequence of Lemma 2.14 that

$$M(G_{n+1}) \simeq \left[\bigvee_{t_{n+1}} S(M(G_n(m_1, \ldots, m_n))) \right] \vee S(M(G_{n-1}(m_1, \ldots, m_{n-1})))$$

for all $n \geq 2$.
   Since both $M(G_{n-1}(m_1, \ldots, m_{n-1}))$ and $M(G_n(m_1, \ldots, m_n))$ are wedges of spheres, using the above equation and Remark 2.11, we obtain

$$A_{n+1,d} = t_{n+1}A_{n,d-1} + A_{n-1,d-1},$$

where recall that $A_{n+1,d}$ is the number of spheres of dimension d in the homotopy type of $M(G_{n+1})$.

Case 2: $(m_{n+1} = 0, m_n \geq 1)$
   We claim that under these assumptions,

$$M(G_{n+1}) \simeq M(G_n(m_1, \ldots, m_n)) \vee S(M(G_{n-1}(m_1, \ldots, m_{n-1})))$$

for all $n \geq 2$.
   To see this, notice that $G_{n+1}(m_1, \ldots, m_n, 0) = G_n(m_1, \ldots, m_{n-1}, m_n+1)$. Using Lemma 2.14, we obtain

$$M(G_{n+1}) = M(G_n(m_1, \ldots, m_n + 1))$$

$$\simeq \left[\bigvee_{(m_n+1)-1} S(M(G_{n-1}(m_1, \ldots, m_{n-1}))) \right] \vee S(M(G_{n-2}(m_1, \ldots, m_{n-2})))$$

$$\simeq \left[\bigvee_{m_n-1} S(M(G_{n-1}(m_1, \ldots, m_{n-1}))) \vee S(M(G_{n-2}(m_1, \ldots, m_{n-2}))) \right] \vee S(M(G_{n-1}(m_1, \ldots, m_{n-1}))).$$

Since $m_n \geq 1$, $m_n - 1 \geq 0$, so we can apply Lemma 2.14 once more to see that

$$\bigvee_{m_n-1} S(M(G_{n-1}(m_1, \ldots, m_{n-1}))) \vee S(M(G_{n-2}(m_1, \ldots, m_{n-2}))) \simeq M(G_n(m_1, \ldots, m_n))$$

It follows that

$$A_{n+1,d} = A_{n,d} + A_{n-1,d-1}.$$

Case 3: $(m_{n+1} = 0, m_n = 0)$
   Consider $G_{n+1}(m_1, \ldots, m_{n-2}, m_{n-1}, 0, 0)$, $n \geq 3$. This graph has an independent 1-leg, so by Lemma 2.14, $M(G_{n+1}) \simeq S(M(G_{n-2}(m_1, \ldots, m_{n-2})))$. Thus in this case,

$$A_{n+1,d} = A_{n-2,d-1}.$$

$\square$

30

Using Theorem 5.13 and the following base cases, we can obtain the homotopy type of any caterpillar graph:

$$M(G_1(m_1)) \simeq \bigvee_{t_1} S^0$$

$$M(G_2(m_1, 0)) = M(G_1(m_1 + 1)) \simeq \bigvee_{t_1 + 1} S^0$$

$$M(G_2(m_1, m_2)) \simeq S^0 \vee (\bigvee_{t_1 t_2} S^1)$$

$$M(G_3(m_1, 0, m_3)) \simeq \bigvee_{t_1 + t_3 + t_1 t_3} S^1$$

where recall that $t_i = m_i - 1$. Using these base cases and the recursions given in Theorem 5.13, one can write code that computes the explicit homotopy type for any caterpillar.

Although there is no known nice formula for general caterpillars, for some families of caterpillar graphs with a pattern of where the zero leg vertices occur, the number of spheres in each dimension does have a nice combinatorial description.

For example, the matching complexes of caterpillar graphs with the property that every other vertex on the central path has zero legs (see Figure 24) are homotopy equivalent to a wedge of spheres in a single dimension. Before we prove this using Theorem 5.13, we will define the following sum that enumerates the number of spheres in the wedge.
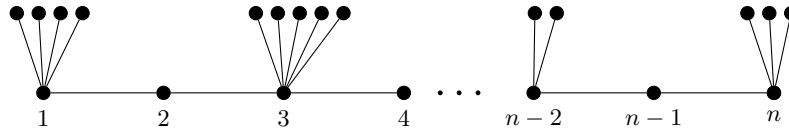

FIGURE 24. A caterpillar graph with the property that every other vertex has zero legs.

Definition 5.14. For $k \geq 0$, let $L_k(a_1, \ldots, a_k)$ denote the following sum:

$$L_k(a_1, \ldots, a_k) = \sum_{\substack{\ell = 1, 2, \ldots, k \\ 1 \leq i_1 < \cdots < i_\ell \leq k}} (i_2 - i_1)(i_3 - i_2) \cdots (i_\ell - i_{\ell-1}) a_{i_1} a_{i_2} \cdots a_{i_\ell}$$

Example 5.15. (Examples of $L_k(a_1, \ldots, a_k)$).
   (1) First consider when $k = 1$. The summand is the single term a_1, corresponding to $i_1 = 1$.
   (2) When $k = 2$ the summand has three terms. For $\ell = 1$ we have a_1 corresponding to $i_1 = 1$ and a_2 corresponding to $i_1 = 2$. For $\ell = 2$ we have $a_1 a_2$ corresponding to $(i_1, i_2) = (1, 2)$. So the resulting sum is $L_2(a_1, a_2) = a_1 + a_2 + (2 - 1)a_1 a_2 = a_1 + a_2 + a_1 a_2$.
   (3) We provide two more examples:
      (i) When $k = 3$, $L_3(a_1, a_2, a_3) = a_1 + a_2 + a_3 + a_1 a_2 + 2a_1 a_3 + a_2 a_3 + a_1 a_2 a_3$
      (ii) When $k = 4$, $L_4(a_1, a_2, a_3, a_4) = a_1 + a_2 + a_3 + a_4 + a_1 a_2 + 2a_1 a_3 + 3a_1 a_4 + a_2 a_3 + 2a_2 a_4 + a_3 a_4 + a_1 a_2 a_3 + 2a_1 a_2 a_4 + 2a_1 a_3 a_4 + a_2 a_3 a_4 + a_1 a_2 a_3 a_4$.

Lemma 5.16. *The polynomials $L_k(a_1, \ldots, a_k)$ satisfy the following relation for $k \geq 2$:*

(3) $$L_k(a_1, \ldots, a_k) = a_k L_{k-1}(a_1, \ldots, a_{k-2}, (a_{k-1} + 1)) + L_{k-1}(a_1, \ldots, a_{k-1}).$$

Proof. Each monomial that appears in equation (3) is of the form $a_{i_1} a_{i_2} \cdots a_{i_\ell}$ where $1 \le \ell \le k$ and $1 \le i_1 < i_2 < \cdots < i_\ell \le k$. We will show that the coefficients of $a_{i_1} a_{i_2} \cdots a_{i_\ell}$ on the left hand side and right hand side of equation (3) are equal. When $i_\ell \le k-1$ the coefficient of $a_{i_1} a_{i_2} \cdots a_{i_\ell}$ arises from $L_{k-1}(a_1, \ldots, a_{k-1})$ on the right hand side which is the same as its coefficient in $L_k(a_1, \ldots, a_k)$ on the left hand side.

Now consider $a_{i_1} a_{i_2} \cdots a_{i_{\ell-1}} a_{i_k}$. If $i_{\ell-1} = k-1$, then the monomial $a_{i_1} a_{i_2} \cdots a_{i_{k-1}} a_{i_k}$ appears on the right hand side of equation (3) only once: when we multiply the term

$$(i_2 - i_1) \cdots (i_{\ell-2} - i_{\ell-3})(k - 1 - i_{\ell-2}) a_{i_1} \cdots a_{i_{\ell-2}} a_{k-1}$$

from the sum $L_{k-1}(a_1, \ldots, a_{k-2}, (a_{k-1}+1))$ by a_k. It also only appears once on the left hand side as the term

$$(i_2 - i_1) \cdots (i_{\ell-2} - i_{\ell-3})(k - 1 - i_{\ell-2})(k - (k-1)) a_{i_1} \cdots a_{i_{\ell-2}} a_{k-1} a_k,$$

as desired.

If $i_{\ell-1} < k-1$, the monomial $a_{i_1} a_{i_2} \cdots a_{i_{\ell-1}} a_k$ appears twice on the right hand side of equation (3). This is because the monomial $a_{i_1} a_{i_2} \cdots a_{i_{\ell-1}}$ appears twice in $L_{k-1}(a_1, \ldots, a_{k-2}, (a_{k-1}+1))$: the term

$$(i_2 - i_1) \cdots (i_{\ell-1} - i_{\ell-2}) a_{i_1} \cdots a_{i_{\ell-1}}$$

and in the term

$$(i_2 - i_1) \cdots (i_{\ell-1} - i_{\ell-2})(k - 1 - i_{\ell-1}) a_{i_1} \cdots a_{i_{\ell-1}} (a_{k-1} + 1)$$

So, the coefficient of $a_{i_1} a_{i_2} \cdots a_{i_{\ell-1}} a_k$ on the right hand side of equation (3) is

$$(i_2 - i_1) \cdots (i_{\ell-1} - i_{\ell-2}) + (i_2 - i_1) \cdots (i_{\ell-1} - i_{\ell-2})(k - 1 - i_{\ell-1}) = (i_2 - i_1) \cdots (i_{\ell-1} - i_{\ell-2})(k - i_{\ell-1})$$

which is equal with its coefficient on the left hand side. $\square$

Caterpillar graphs with the property that every other vertex on the central path has zero legs can always be written $G_k^a := G_{2k-1}(m_1, 0, m_2, 0, \ldots, m_{k-1}, 0, m_k)$. For if we have a caterpillar on $2k$ vertices of the form $G_{2k}(m_1, 0, m_2, 0, \ldots, m_{k-1}, 0, m_k, 0)$, we could rewrite this as a caterpillar on $2k - 1$ vertices: $G_{2k-1}(m_1, 0, m_2, 0, \ldots, m_{k-1}, 0, m_k + 1)$. So in a caterpillar graph denoted G_k^a, the number of vertices on the central path is always odd.

With this notation, m_i is the number of legs on the $(2i - 1)$-th vertex of the central path, rather than the ith vertex of the central path. While this is not consistent with the notation in Theorem 5.13, it simplifies the statement and proof that follows.

Theorem 5.17. *Let $G_k^a = G_{2k-1}(m_1, 0, m_2, 0, \ldots, m_{k-1}, 0, m_k)$ be a caterpillar graph such that vertices $2, 4, \ldots, 2k - 2$ on the central path have degree 2, and vertices $1, 3, \ldots, 2k - 1$ have m_i legs ($m_i \ge 1$). Then, for $k \in \mathbb{N}$, the homotopy type of $M(G_k^a)$ is given by:*

$$M(G_k^a) \simeq \bigvee_{L_k(a_1, a_2, \ldots, a_k)} S^{k-1}$$

where $a_i = m_i - 1$ for $i = 1, \ldots, k$.

Proof. We will prove the theorem by induction on k. When $k = 1$, $M(G_1(m_1))$ is a discrete set of m_1 points, so $M(G_1) = \bigvee_{a_1} S^0$ where $a_1 = m_1 - 1$ as desired.

Now assume the claim holds for $1, \ldots, k - 1$ and consider $G_{2k-1}(m_1, 0, m_2, 0, \ldots, m_k)$. Since $m_k \ge 1$, by Theorem 5.13,

$$A_{2k-1,d} = a_k A_{2k-2,d-1} + A_{2k-3,d-1}$$

where recall that $A_{2k-1,d}$ is the number of spheres of dimension d in $G_{2k-1}(m_1, 0, m_2, 0, \ldots, m_k)$, $A_{2k-2,d-1}$ is the number of spheres of dimension $d-1$ in $G_{2k-2}(m_1, 0, m_2, 0, \ldots, m_{k-1}, 0)$ and $A_{2k-3,d-1}$ is the number of spheres of dimension $d-1$ in $G_{2k-3}(m_1, 0, m_2, 0, \ldots, m_{k-1})$. Using the induction hypothesis and the fact that

$$G_{2k-2}(m_1, 0, m_2, 0, \ldots, m_{k-1}, 0) = G_{2k-3}(m_1, 0, m_2, 0, \ldots, m_{k-1} + 1)$$

we see that $A_{2k-2,d-1} = L_{k-1}(a_1, a_2, \ldots, (a_{k-1} + 1))$ and $A_{2k-3,d-1} = L_{k-1}(a_1, a_2, \ldots, a_{k-1})$ if $d = k - 1$ and $A_{2k,d-1} = A_{2k-1,d-1} = 0$ otherwise. So by Lemma 5.16, $A_{2k+1,d} = L_k(a_1, a_2, \ldots, a_k)$ if $d = k - 1$ and 0 otherwise, as desired. $\qquad\square$

6. Future Directions

In Section 4, we explored the matching complexes of honeycomb graphs and partially answered a question posed by Jonsson [21] by presenting a weak lower bound for connectivity of an $r \times s \times t$ honeycomb graph and sharper bounds in the cases when $r = s = 1$ and $r = 2$, $s = 1$. The work to understand these complexes is far from done.

We saw in Remark 4.8 that while a natural conjecture may be that the connectivity of the matching complex is at least one less than the number of hexagons, this does not turn out to be true. This raises the question:

Question 6.1. What is the connectivity of $r \times s \times t$ honeycomb graphs, where $r \geq 3, s \geq 1$, and $t \geq 1$?

In the introduction we also discussed Kekulé structures, which are perfect matchings of a honeycomb graph that have been studied in chemistry [22, 19]. Perfect matchings of a honeycomb graph are the maximal dimensional faces of the matching complex, so we can consider the subcomplex induced by these faces, leading us to ask:

Question 6.2. What is the relationship between matching complexes of honeycomb graphs and Kekulé structures?

In Section 5, we turned our attention to trees and saw that the homotopy type of forests is either a point or a wedge of spheres. Consequently, acyclic graphs do not contain torsion. From work by Shareshian and Wachs [30] and Jonnson [21], we know that torsion appears in higher homology groups of the full matching complex $M(K_n)$ and the chessboard complex $M(K_{m,n})$. It would be interesting to determine if there is torsion in the higher homology groups of honeycomb graphs.

Question 6.3. Is there torsion in the matching complexes of $r \times s \times t$ honeycomb graphs?

While we gave the explicit homotopy type of caterpillar graphs in Section 5.1, we were unable to determine the number of spheres in each dimension for other types of trees. Thus the following question remains unanswered.

Question 6.4. What is the explicit homotopy type of matching complexes of trees?

One avenue of exploration for this problem would be to build a program in Sage that uses Lemma 2.14 to recursively compute the homotopy type of matching complexes of general trees.

Our results for caterpillar graphs suggest that it may be useful to continue to first study specific families of trees, such as *perfect binary trees*. A perfect binary tree is a rooted tree in which every non-leaf vertex has two children. The *depth* of a node in a binary tree is the

number of edges in the path from that node to the root and the *height* of a binary tree is the depth of a leaf. A perfect binary tree of height h has 2^h leaves.

Example 6.5. Let T_h denote a perfect binary tree of height h. T_1 is P_3, so $M(T_1) = S^0$. $M(T_2) \simeq S^1 \vee S^1 \vee S^1$. Using Lemma 2.14 and Theorem 5.11, we find that $M(T_3) \simeq S^4 \bigvee \left[\bigvee_4 S^3 \right]$.

Using homology tools in Sage in conjunction with Theorem 5.1, $M(T_4) \simeq \bigvee_{56} S^8 \vee \bigvee_{11} S^9$.

Proposition 6.6. *Let T_h be a perfect binary tree with height $h \geq 3$ and let $L = \lceil \frac{h}{3} \rceil - 1$. Then $M(T_h)$ is at least $((\sum_{i=0}^{L} 2^{h-3i-1}) - 2)$-connected.*

Proof. Let T_h be a perfect binary tree of height h. The line graph of T_h is made up of $h - 1$ rows of triangles such that there are 2^{h-k} triangles in the kth row, where the rows are numbered 1 to $h - 1$ from bottom to top (see Figure 25). For $k \equiv 1 \bmod 3$, we label the lower left vertex of each triangle in the kth row v_i^j, where $j = \frac{k+2}{3}$ and i ranges from 1 to 2^{h-k} moving from left to right. If $h \equiv 1 \bmod 3$, we also label the top left vertex v_1^j where $j = \frac{h+2}{3}$. In total, this gives us $\sum_{i=0}^{L} 2^{h-3i-1}$ labeled vertices where $L = \lceil \frac{h}{3} \rceil - 1$.

Because the distance between any pair of labeled vertices is at least three, they satisfy the conditions of Lemma 2.8. Thus, all critical cells have at least $\sum_{i=0}^{L} 2^{h-3i-1}$ elements and $M(T_h)$ must be at least $((\sum_{i=0}^{L} 2^{h-3i-1}) - 2)$-connected.

$\square$

The bound given here improves the general bounds given by Barmak [2, Theorem 5.5] and Engström [13, Theorem 3.2] for this specific case. Recall from Section 4 that Engström's bound is based on the maximum degree and number of vertices of the line graph. For the symmetric binary tree of height h the maximum degree is 3 and the number of vertices in the line graph is $\sum_{k=1}^{h} 2^k$. Therefore, Theorem 3.2 in [13] yields a connectivity bound of $\lfloor \frac{2}{11} \sum_{k=1}^{h} 2^k - \frac{12}{11} \rfloor$. The bound provided by Barmak is based on the dimension of $M(T_h)$ which is given by $\sum_{k=0}^{\lfloor \frac{h-1}{2} \rfloor} \frac{2^{h-2k}}{2} - 1$. It follows that Theorem 5.5 in [2] yields a connectivity bound of $\sum_{k=0}^{\lfloor \frac{h-1}{2} \rfloor} \frac{2^{h-2k}}{4} - \frac{3}{2}$. In both cases, when h is a positive integer, the connectivity bound provided in Proposition 6.6 provides an improved result. Although it is not clear if this bound is the best possible, for the small examples given in Example 6.5 the bound given by the proposition is the best possible lower bound. We leave the reader with a final question:

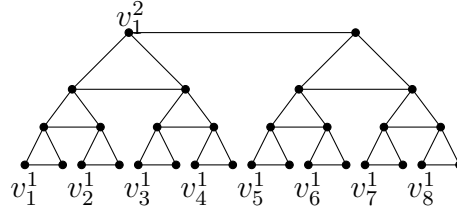**Question 6.7.** Is the connectivity bound given in Proposition 6.6 tight?

FIGURE 25. The line graph of a perfect binary tree of height 4 $L(T_4)$.

References

[1] Michal Adamaszek. Splittings of independence complexes and the powers of cycles. *J. Combin. Theory Ser. A*, 119(5):1031–1047, 2012.

[2] Jonathan Ariel Barmak. Star clusters in independence complexes of graphs. *Adv. Math.*, 241:33–57, 2013.

[3] Margaret Bayer, Bennet Goeckner, and Marija Jelić Milutinović. Manifold Matching Complexes. arXiv:1906.03328 [math.CO].

[4] A. Björner, L. Lovász, S. T. Vrećica, and R. T. Živaljević. Chessboard complexes and matching complexes. *J. London Math. Soc. (2)*, 49(1):25–39, 1994.

[5] Anders Björner, Michelle L. Wachs, and Volkmar Welker. Poset fiber theorems. *Trans. Amer. Math. Soc.*, 357(5):1877–1899, 2005.

[6] S. Bouc. Homologie de certains ensembles de 2-sous-groupes des groupes symétriques. *J. Algebra*, 150(1):158–186, 1992.

[7] Mireille Bousquet-Mélou, Svante Linusson, and Eran Nevo. On the independence complex of square grids. *J. Algebraic Combin.*, 27(4):423–450, 2008.

[8] Benjamin Braun. Independence complexes of stable Kneser graphs. *Electron. J. Combin.*, 18(1):Paper 118, 17, 2011.

[9] Benjamin Braun and Wesley K. Hough. Matching and independence complexes related to small grids. *Electron. J. Combin.*, 24(4):Paper 4.18, 20, 2017.

[10] Kenneth S. Brown. Euler characteristics of discrete groups and G-spaces. *Invent. Math.*, 27:229–264, 1974.

[11] Kenneth S. Brown. Euler characteristics of groups: the p-fractional part. *Invent. Math.*, 29(1):1–5, 1975.

[12] Boris Bukh. Topological methods in combinatorics: on wedges and joins. Lecture notes available at http://www.borisbukh.org/TopCombLent12/notes wedgejoin.pdf.

[13] Alexander Engström. Independence complexes of claw-free graphs. *European J. Combin.*, 29(1):234–241, 2008.

[14] Alexander Engström. Complexes of directed trees and independence complexes. *Discrete Math.*, 309(10):3299–3309, 2009.

[15] Robin Forman. A user's guide to discrete Morse theory. *Sém. Lothar. Combin.*, 48:Art. B48c, 35, 2002.

[16] Joel Friedman and Phil Hanlon. On the Betti numbers of chessboard complexes. *Journal of Algebraic Combinatorics*, 8(2):193–203, 1998.

[17] Peter Freedman Garst. *Cohen-Macaulay Complexes and group actions.* ProQuest LLC, Ann Arbor, MI, 1979. Thesis (Ph.D.)–The University of Wisconsin - Madison.

[18] Allen Hatcher. *Algebraic topology.* Cambridge University Press, Cambridge, 2002.

[19] GE Hite, TP Živković, and DJ Klein. Conjugated circuit theory for graphite. *Theoretica chimica acta*, 74(5):349–361, 1988.

[20] Jakob Jonsson. Matching complexes on grids. unpublished manuscript available at http://www.math.kth.se/~jakobj/doc/thesis/grid.pdf.

[21] Jakob Jonsson. *Simplicial complexes of graphs*, volume 1928 of *Lecture Notes in Mathematics*. Springer-Verlag, Berlin, 2008.

[22] DJ Klein, GE Hite, WA Seitz, and TG Schmalz. Dimer coverings and Kekulé structures on honeycomb lattice strips. *Theoretica chimica acta*, 69(5-6):409–423, 1986.

[23] Dmitry Kozlov. *Combinatorial algebraic topology*, volume 21 of *Algorithms and Computation in Mathematics*. Springer, Berlin, 2008.

[24] Dmitry N. Kozlov. Complexes of directed trees. *J. Combin. Theory Ser. A*, 88(1):112–122, 1999.

[25] Greg Kuperberg. Symmetries of plane partitions and the permanent-determinant method. *J. Combin. Theory Ser. A*, 68(1):115–151, 1994.

[26] Mario Marietti and Damiano Testa. Cores of simplicial complexes. *Discrete Comput. Geom.*, 40(3):444–468, 2008.

[27] Mario Marietti and Damiano Testa. A uniform approach to complexes arising from forests. *Electron. J. Combin.*, 15(1):Research Paper 101, 18, 2008.

[28] Takahiro Matsushita. Matching complexes of small grids. *Electron. J. Combin.*, 26(3):Paper 3.1, 8, 2019.

[29] Daniel Quillen. Homotopy properties of the poset of nontrivial p-subgroups of a group. *Adv. in Math.*, 28(2):101–128, 1978.

[30] John Shareshian and Michelle L. Wachs. Torsion in the matching complex and chessboard complex. *Adv. Math.*, 212(2):525–570, 2007.

[31] Richard P. Stanley. Symmetries of plane partitions. *J. Combin. Theory Ser. A*, 43(1):103–113, 1986.

[32] Rade T. Živaljević and Siniša T. Vrećica. The colored Tverberg's problem and complexes of injective functions. *J. Combin. Theory Ser. A*, 61(2):309–318, 1992.

[33] Michelle L. Wachs. Topology of matching, chessboard, and general bounded degree graph complexes. *Algebra Universalis*, 49(4):345–385, 2003. Dedicated to the memory of Gian-Carlo Rota.

[34] George W. Whitehead. Homotopy groups of joins and unions. *Trans. Amer. Math. Soc.*, 83:55–69, 1956.

[35] Russ Woodroofe. Vertex decomposable graphs and obstructions to shellability. *Proc. Amer. Math. Soc.*, 137(10):3235–3246, 2009.

[36] Günter M. Ziegler. Shellability of chessboard complexes. *Israel J. Math.*, 87(1-3):97–110, 1994.

FACULTY OF MATHEMATICS, UNIVERSITY OF BELGRADE, BELGRADE, SERBIA
E-mail address: marijaj@matf.bg.ac.rs

DEPARTMENT OF MATHEMATICS, UNIVERSITY OF OREGON, EUGENE, OR 97403–1222
E-mail address: hjenne@uoregon.edu

DEPARTMENT OF MATHEMATICS, BROWN UNIVERSITY, PROVIDENCE, RI 02912–9032
E-mail address: amcd@math.brown.edu

DEPARTMENT OF MATHEMATICS, UNIVERSITY OF KENTUCKY, LEXINGTON, KY 40506–0027
E-mail address: julianne.vega@uky.edu

Dim / Tree	0	1	2	3	4	5	6	7
$G_1(m_1)$	t_1	0						
$G_2(m_1,m_2)$	1	t_1t_2						
$G_3(m_1,m_2,m_3)$	0	t_1+t_3	$t_1t_2t_3$					
$G_4(m_1,\ldots,m_4)$	0	1	$t_1t_2+t_1t_4+t_3t_4$	$t_1t_2t_3t_4$				
$G_5(m_1,\ldots,m_5)$	0	0	$t_1+t_3+t_5$	$t_1t_2t_3 + t_1t_2t_5 + t_1t_4t_5 + t_3t_4t_5$	$t_1t_2t_3t_4t_5$			
$G_6(m_1,\ldots,m_6)$	0	0	1	$t_1t_2+t_1t_4+t_3t_4+ t_1t_6+t_3t_6+t_5t_6$	$t_1t_2t_3t_4 + t_1t_2t_3t_6 + t_1t_2t_5t_6 + t_1t_4t_5t_6 + t_3t_4t_5t_6$	$t_1t_2t_3t_4t_5t_6$		
$G_7(m_1,\ldots,m_7)$	0	0	0	$t_1 + t_3 + t_5 + t_7$	$t_1t_2t_3 + t_1t_2t_5 + t_1t_4t_5 + t_3t_4t_5 + t_1t_2t_7 + t_1t_4t_7 + t_1t_2t_7 + t_1t_6t_7 + t_3t_4t_7 + t_1t_6t_7 + t_3t_6t_7 + t_5t_6t_7$	$t_1t_2t_3t_4t_5 + t_1t_2t_3t_4t_7 + t_1t_2t_3t_6t_7 + t_1t_2t_5t_6t_7 + t_1t_4t_5t_6t_7 + t_3t_4t_5t_6t_7$	$t_1t_2t_3t_4t_5t_6t_7$	

TABLE 1. The number of spheres of dimension d in the homotopy type of $M(G_n(m_1,\ldots,m_n))$, where $G_n(m_1,\ldots,m_n)$ is a caterpillar with $m_i = t_i + 1$ legs at each vertex i of the central path.